UNITED NATIONS EDUCATIONAL, SCIENTIFIC AND CULTURAL ORGANIZATION
INTERNATIONAL ATOMIC ENERGY AGENCY
INTERNATIONAL CENTRE FOR THEORETICAL PHYSICS
I.C.T.P., P.O. BOX 586, 34100 TRIESTE, ITALY, CABLE: CENTRATOM TRIESTE

H4.SMR/1013-26

SCHOOL ON THE USE OF SYNCHROTRON RADIATION IN SCIENCE AND TECHNOLOGY:
"John Fuggle Memorial"

3 November - 5 December 1997

Miramare - Trieste, Italy

Electromagnetic Interaction with Matter

A. Baldereschi
University of Trieste
Italy

ELECTROMAGNETIC INTERACTION WITH MATTER

A. Baldereschi

Department of Theoretical Physics
University of Trieste, Italy

and

Institut de Physique Appliquée
Ecole Polytechnique Fédérale de Lausanne, Switzerland

Contents:

Adiabatic approximation (to handle a system of electrons $[i = 1, \dots, N]$ and nuclei $[\nu = 1, \dots, N']$)

$$H = T_e + V_{ee} + V_{en} + T_n + V_{nn}$$

$T \equiv$ kinetic energy

$V \equiv$ potential energy

where:

$$T_e = \sum_{i=1}^{N} \frac{p_i^2}{2m} \qquad T_n = \sum_{\nu=1}^{N'} \frac{P_\nu^2}{2M_\nu}$$

$$V_{en} = \sum_{i=1}^{N} \sum_{\nu=1}^{N'} \frac{-Z_\nu e^2}{|r_i - R_\nu|}$$

$$V_{ee} = \frac{1}{2} \sum_{i,j=1}^{N}{}' \frac{e^2}{|r_i - r_j|} \qquad V_{nn} = \frac{1}{2} \sum_{\nu,\mu=1}^{N'}{}' \frac{Z_\nu Z_\mu e^2}{|R_\nu - R_\mu|}$$

Two adiabatic eigenvalue problems are obtained: the first is for electrons

(I) $$H_e \, \varphi_\ell(r; R) = \left[T_e + V_{ee} + V_{en} + V_{nn} \right] \varphi_\ell(r; R) =$$

$$= \varepsilon_\ell(R) \, \varphi_\ell(r; R)$$

and the second for the nuclei

(II) $$H_n^{(\ell)} \chi_{\lambda\ell}(R) = \left[T_n + \varepsilon_\ell(R) \right] \chi_{\lambda\ell}(R) =$$

$$= E_{\lambda\ell} \, \chi_{\lambda\ell}(R)$$

ELECTRONS IN CRYSTALS

Density-functional Kohn-Sham theory

"Real" crystal (interacting electrons)

$$H_e(N) = \sum_{i=1}^{N}\left[\frac{p_i^2}{2m} + v(r_i)\right] + \frac{1}{2}\sum_{i,j=1}^{N}\frac{e^2}{r_{ij}} + \frac{1}{2}\sum_{k,\ell=1}^{N'}\frac{Z_k Z_\ell e^2}{R_{k\ell}}$$

$$v(\vec{r}) = \sum_{k=1}^{N'}\frac{-Z_k e^2}{|\vec{r} - \vec{R}_k|}$$

Equivalent Kohn-Sham system (non-interacting electrons with same particle density)

$$\tilde{H}(N) = \sum_{i=1}^{N}\left[\frac{p_i^2}{2m} + v_{eff}(\vec{r}_i)\right] + \frac{1}{2}\sum_{k,\ell=1}^{N'}\frac{Z_k Z_\ell e^2}{R_{k\ell}}$$

$$\begin{cases} v_{eff}(\vec{r}) = v(\vec{r}) + v_H(\vec{r}) + v_{xc}(\vec{r}) \\ v_H(\vec{r}) = e^2\int\frac{n(\vec{r}')}{|\vec{r}-\vec{r}'|}\,d^3r' \\ v_{xc}(\vec{r}) = F[n(\vec{r})] = \frac{\delta E_{xc}[n]}{\delta n(\vec{r})} \end{cases}$$

STANDARD BAND-STRUCTURE SCHEME

for solving the Kohn - Sham equations.

1. $\tilde{H}\ \Psi_{m,k}(\mathbf{r}) = \varepsilon_m(\mathbf{k})\ \Psi_{m,k}(\mathbf{r})$

$$\tilde{H} = \frac{p^2}{2m} + V_n(\mathbf{r}) + V_e(\mathbf{r}) \longrightarrow v_{eff}(\vec{r})$$

$$V_e(\mathbf{r}) = V_H(\mathbf{r}) + V_{xc}(\mathbf{r})$$

2. $$\rho(\mathbf{r}) = e \sum_{m,k} |\Psi_{m,k}(\mathbf{r})|^2$$

3a. $$V_{xc}(\mathbf{r}) = F[\rho(\mathbf{r})]$$

3b. $$\Delta V_H(\mathbf{r}) = -4\pi e\, \rho(\mathbf{r})$$

which implies two constants of integration.

Standard scheme sets:

(i) $$\int_\Omega \nabla V_H(\mathbf{r})\, d^3r = \langle E \rangle = 0$$

(ii) $$\int_\Omega V_H(\mathbf{r})\, d^3r = \langle V_H \rangle = 0.$$

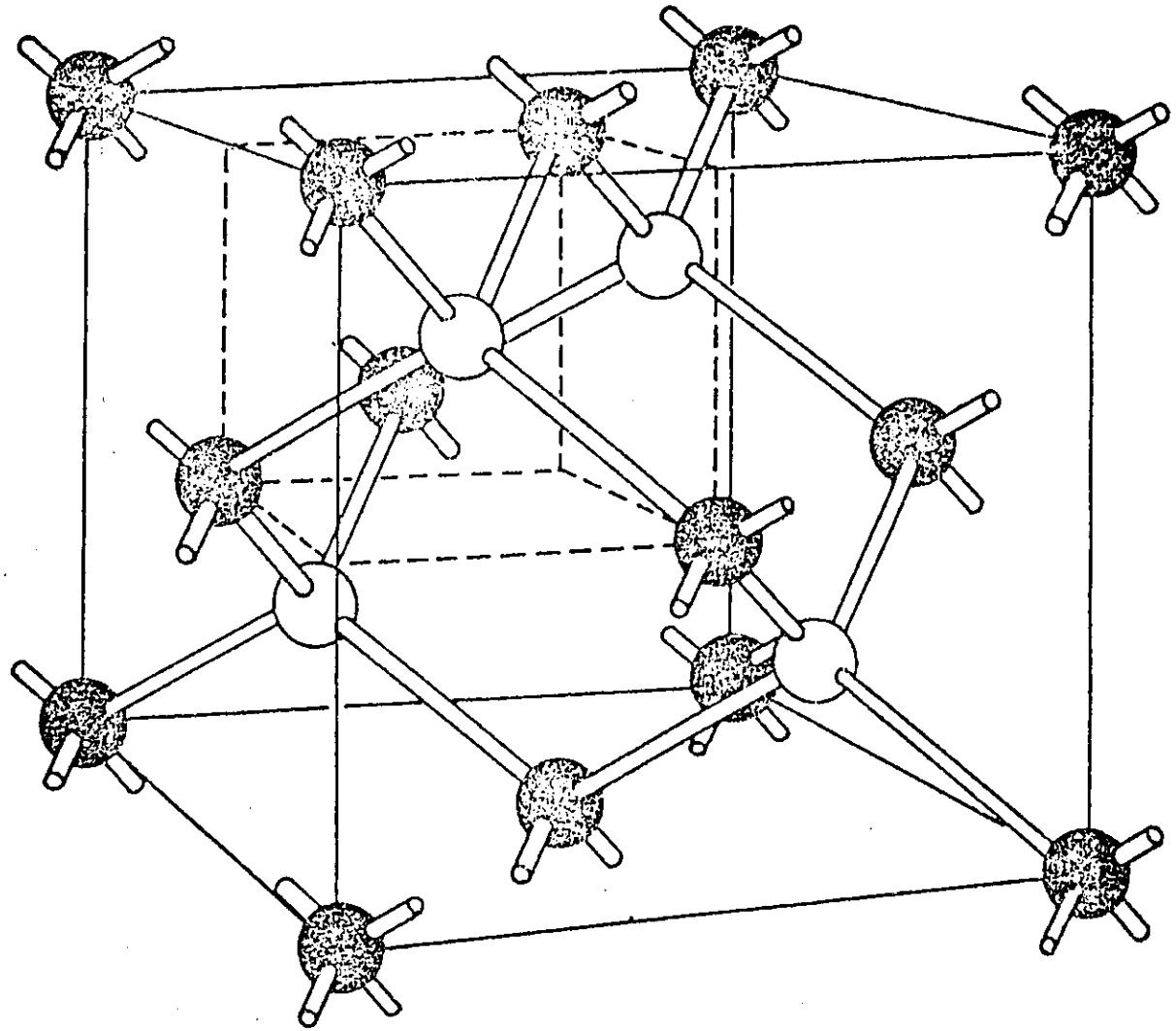

Zinc-blende crystal lattice.

Each atom has tetrahedral coordination (4 neighbors).
Applies to most cubic semiconductors (GaAs, InAs, InP, ZnS

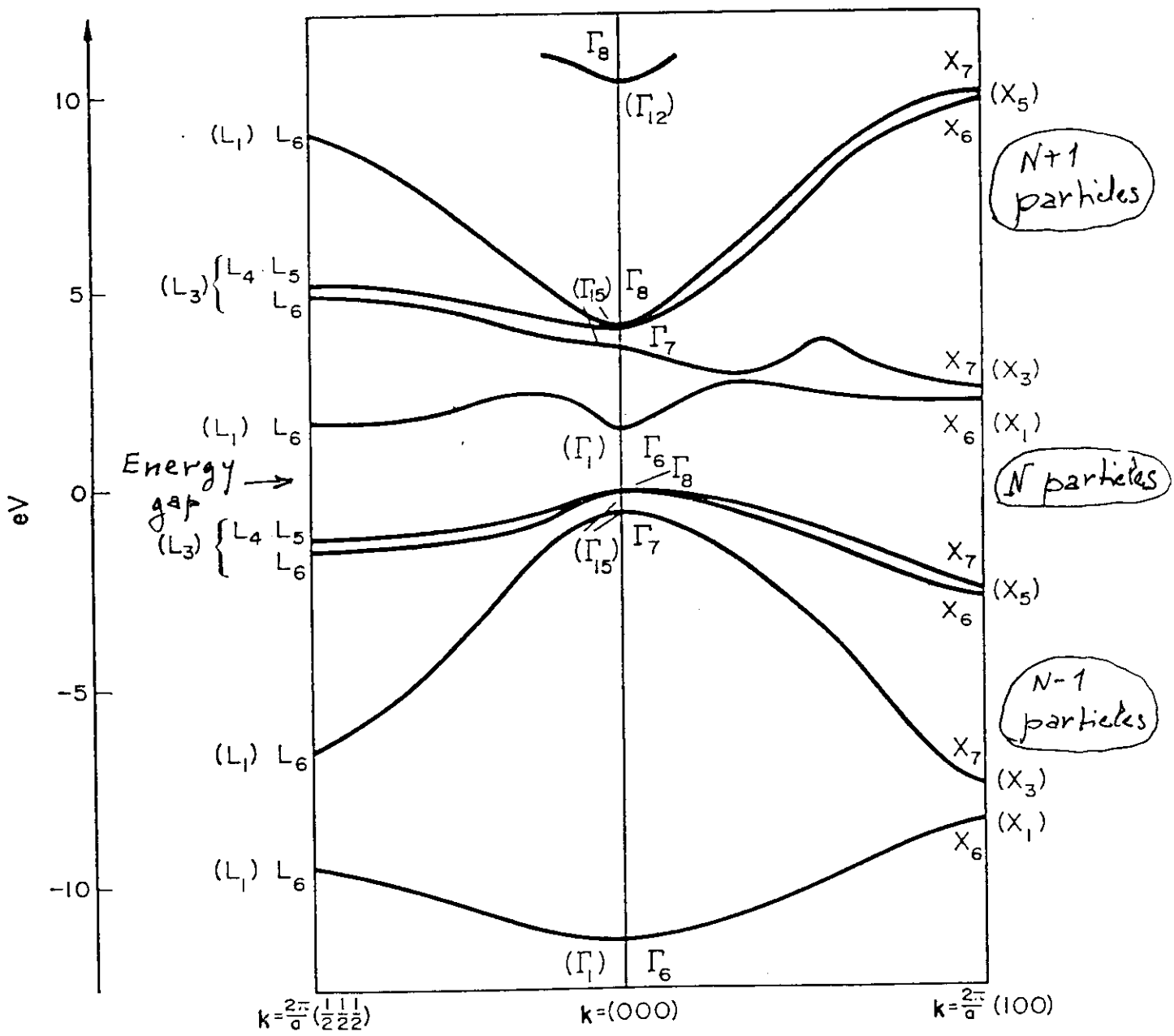

Energy bands for GaAs with the inclusion of spin–orbit interaction. The irreducible representations for the states of the simple group are supplied in brackets.

Valence - band density of states for crystal - GaAs and amorphous - GaAs measured by UPS. Notice similarity.

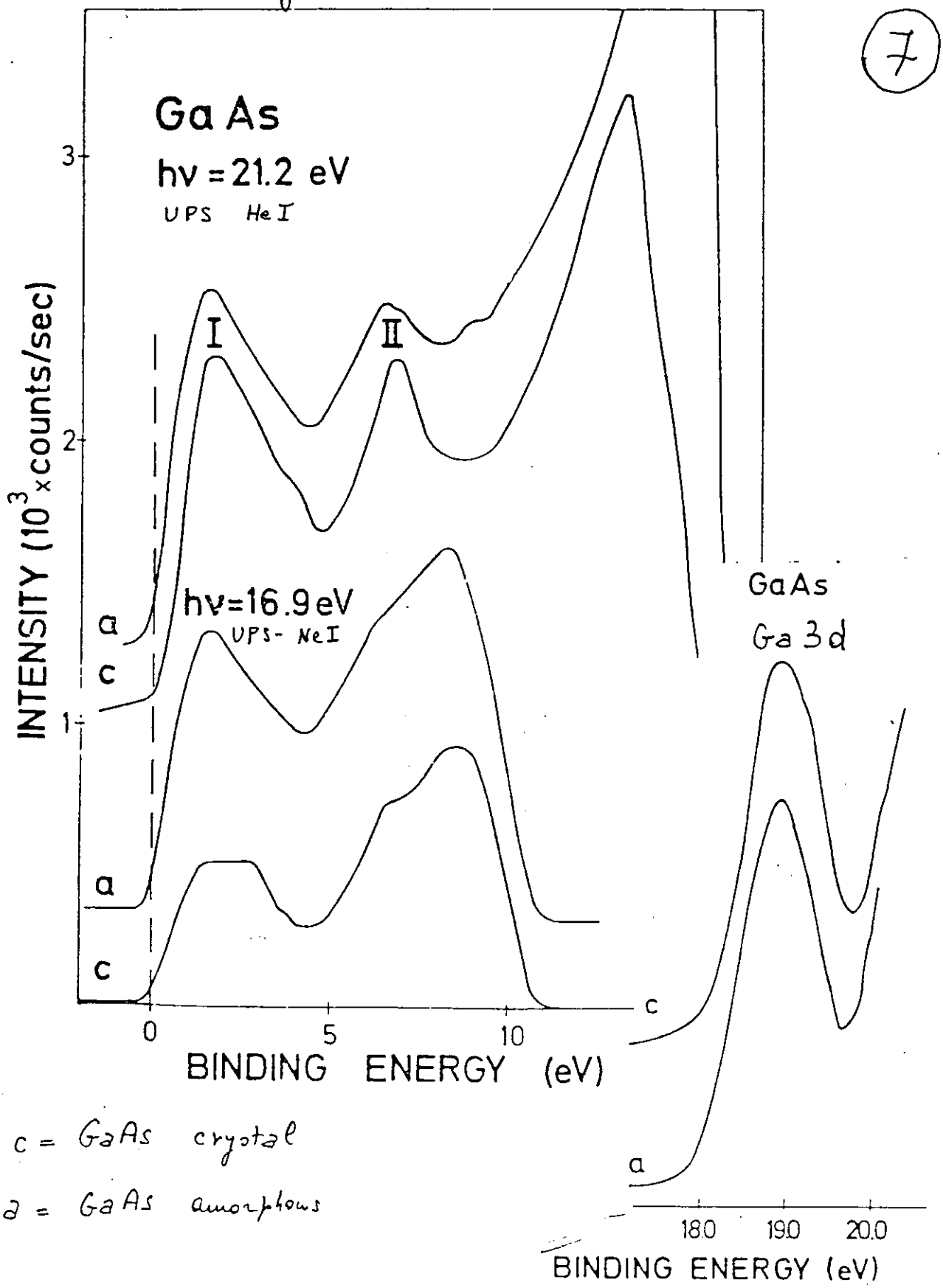

7

c = GaAs crystal

a = GaAs amorphous

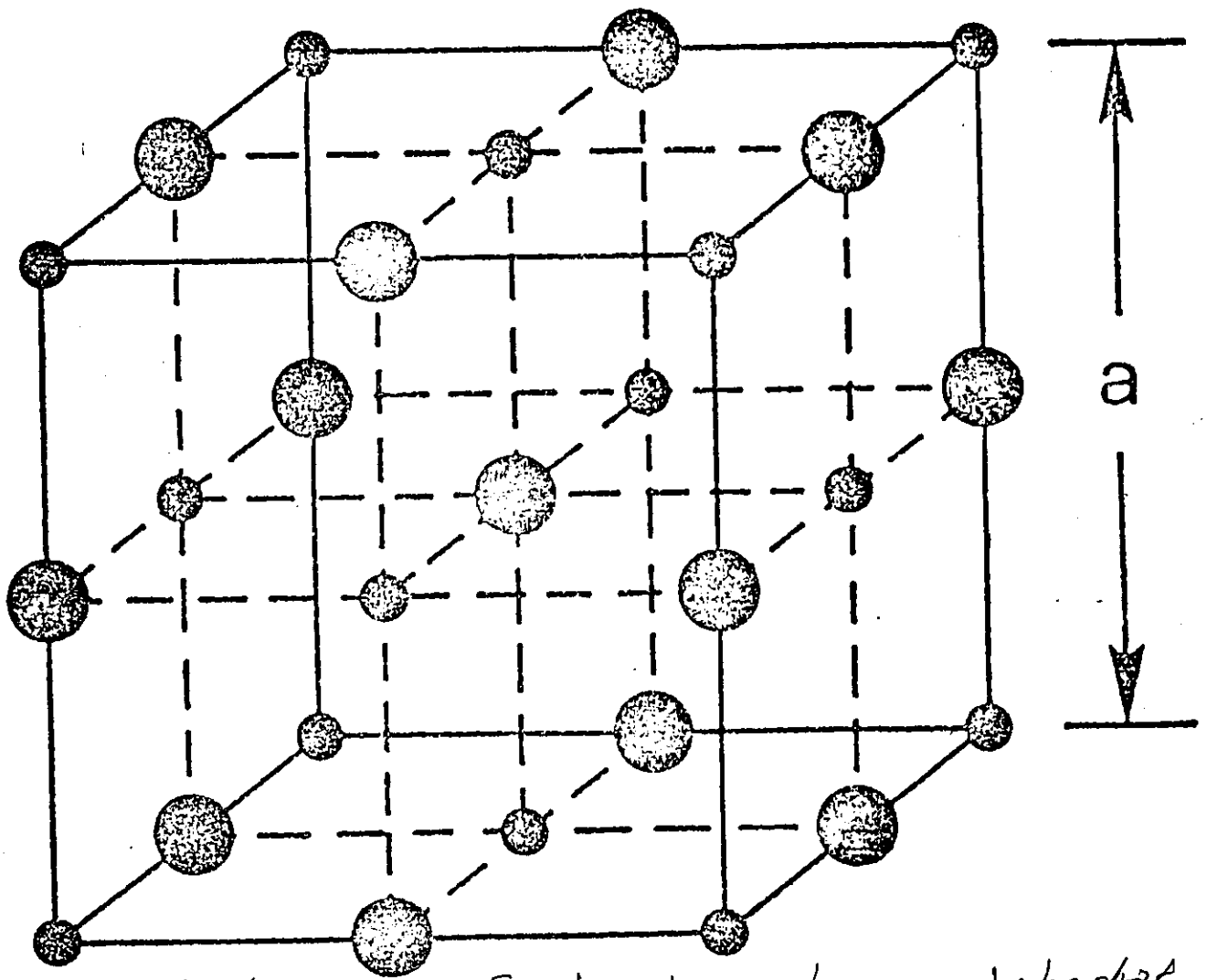

Rock salt crystal lattice. Each atom has octahedral coordinatio
(6 neighbours). Applies to many ionic solids (MgO, $NaCl$, NiO, ...)

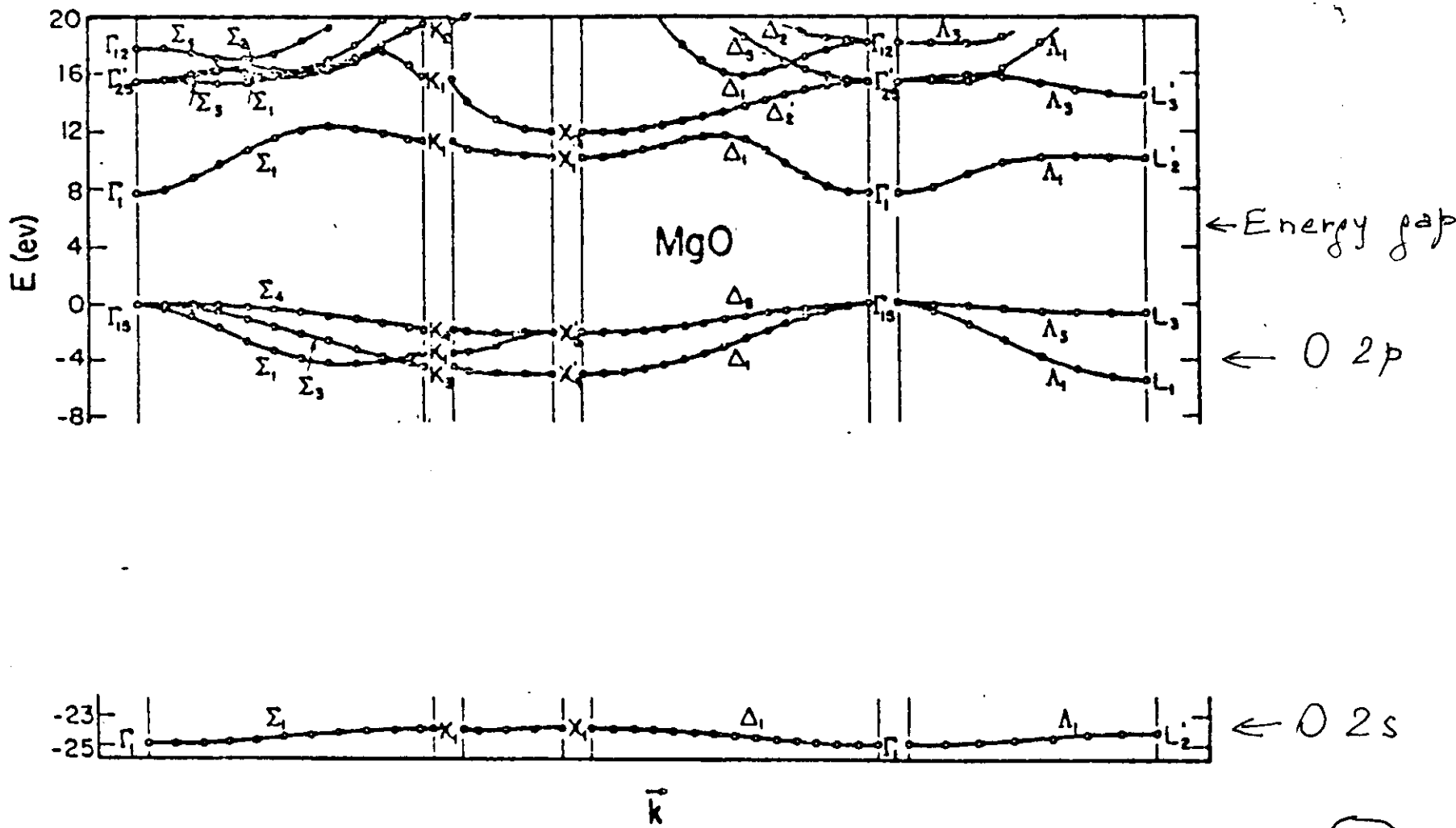

Electronic energy band structure of MgO.

Spin-orbit interaction is not included.

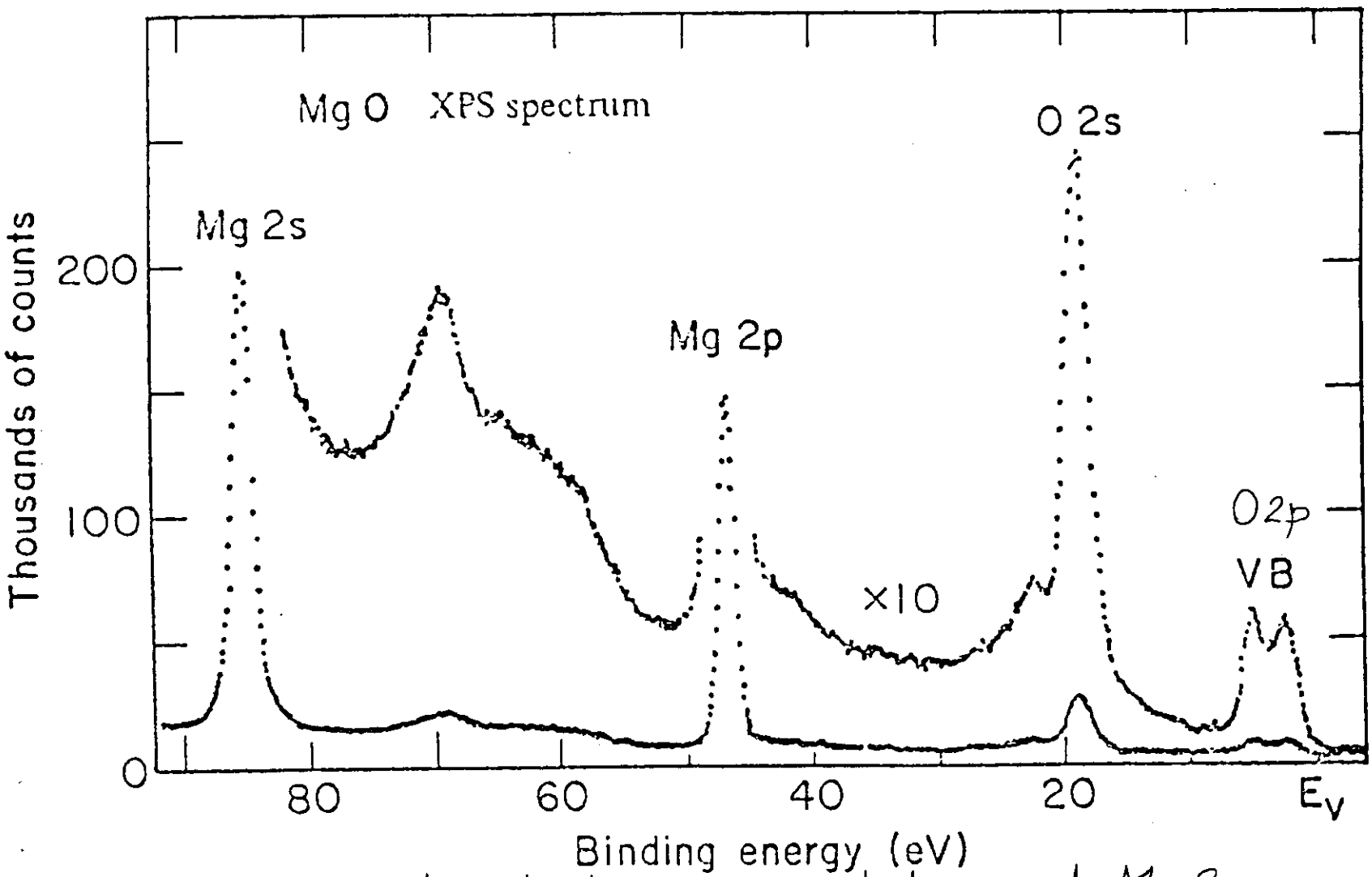

Valence- and core-band density of states of MgO measured by XPS. Upper valence band (VB) corresponds to O2p bands.

(10)

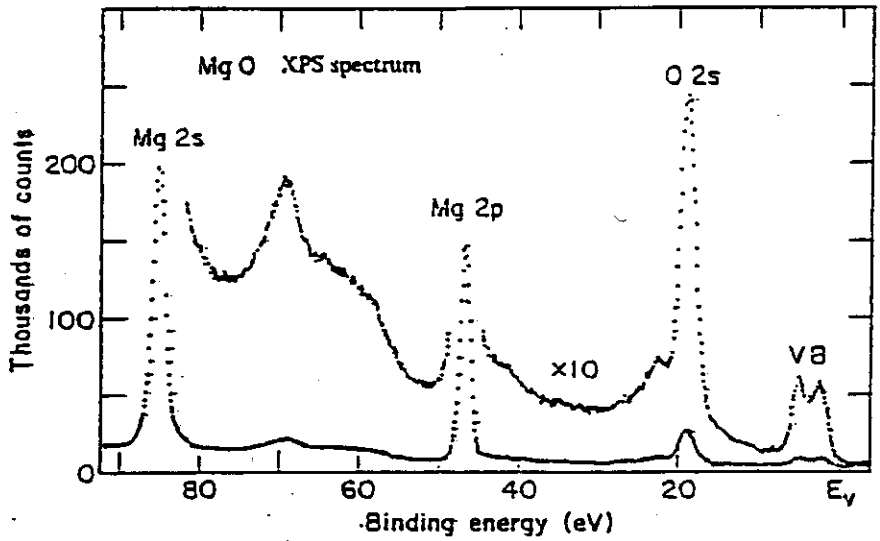

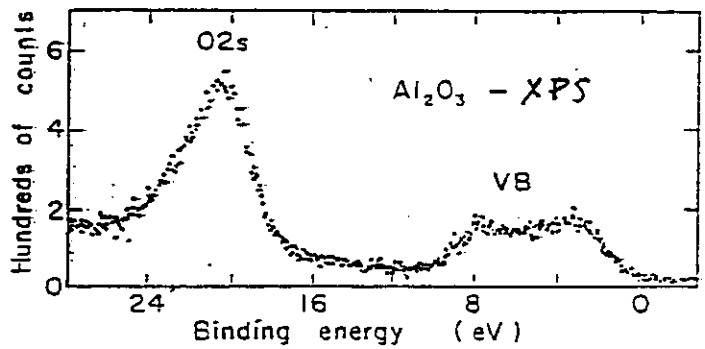

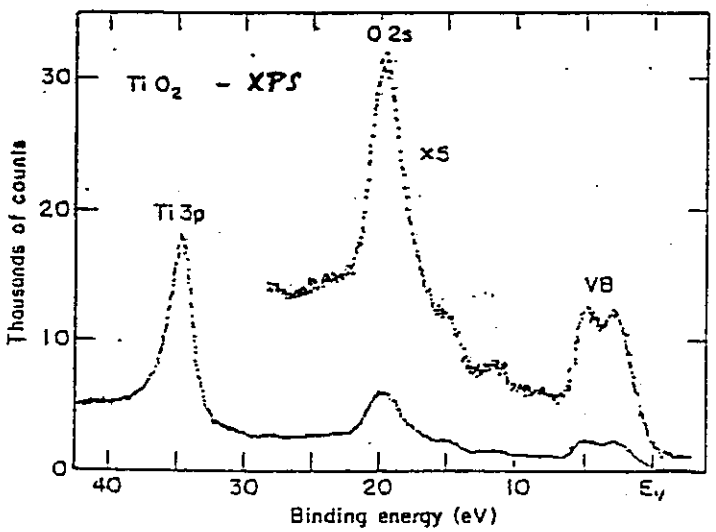

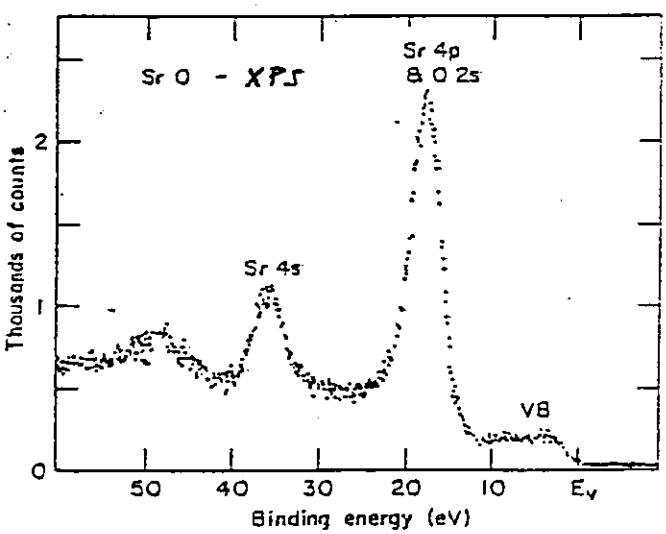

Al Kα XPS spectra of several oxides

Notice similarity of O2s and O2p structures in different compounds.

Total and partial (atomic) density of states in NiO - Spin ↑ states only are represented.

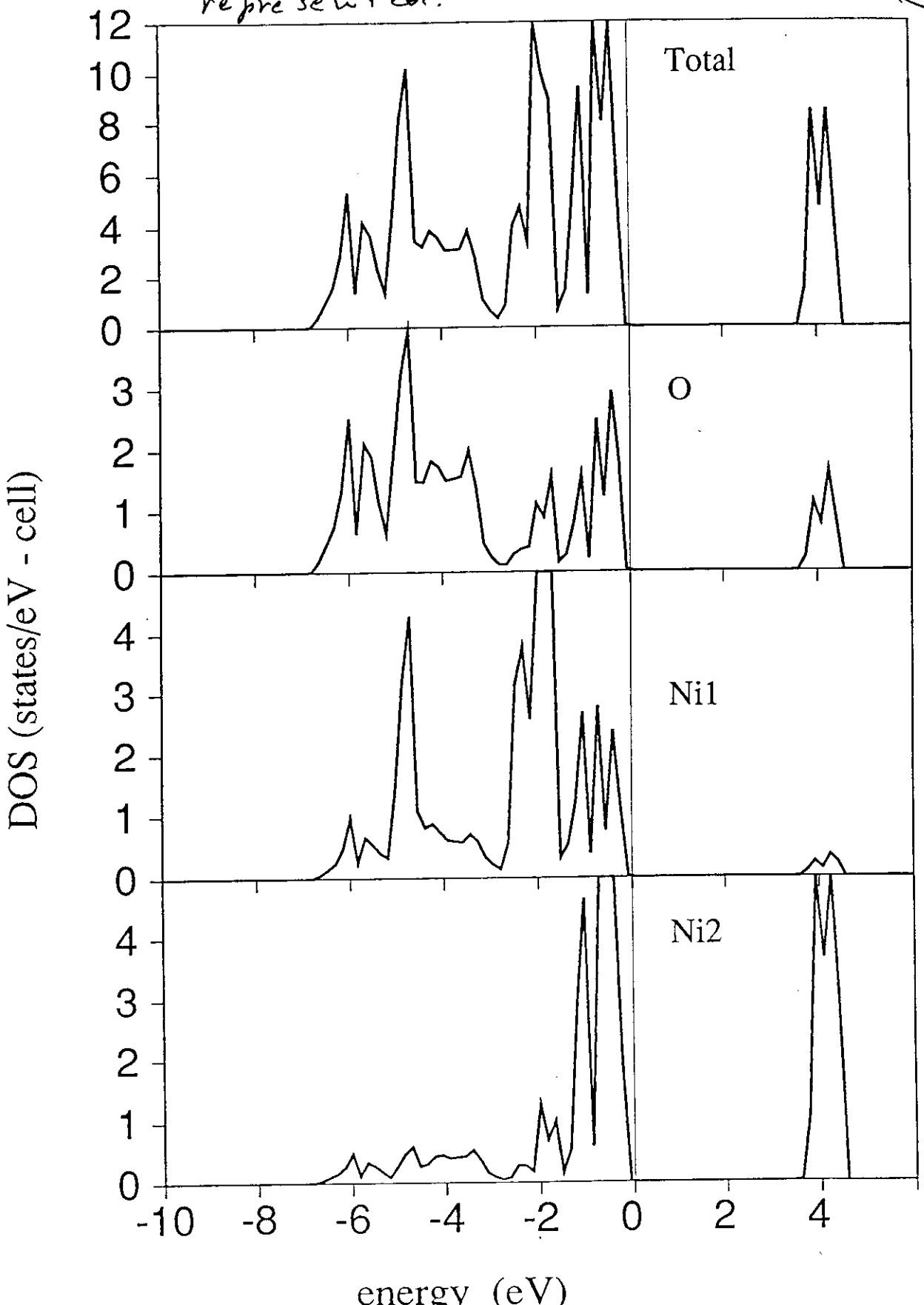

Theoretical Density of states of NiO for both occupied ($E<0$) and empty states ($E>0$).

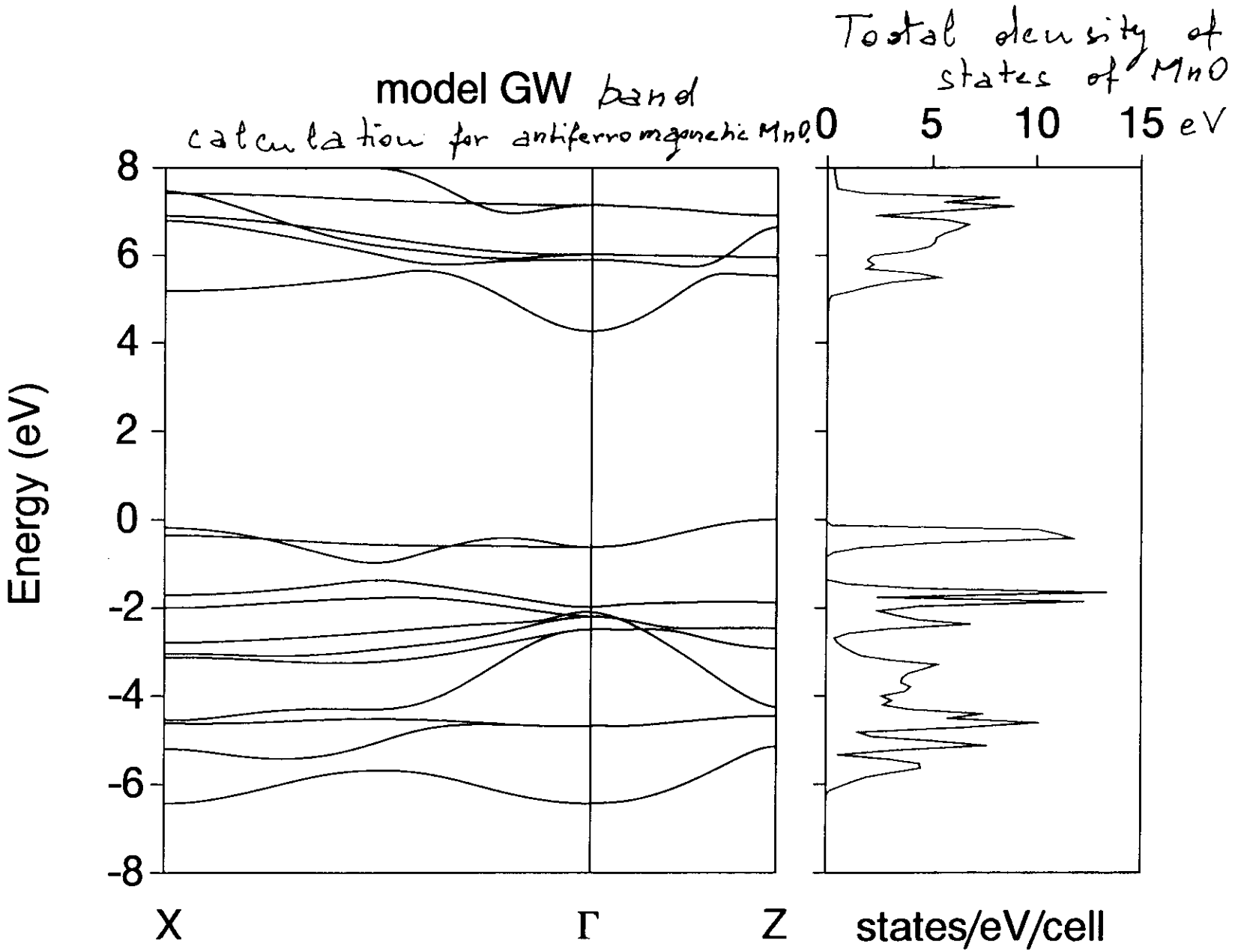
model GW band
calculation for antiferromgnetic MnO
Total density of states of MnO
0
5
10
15 eV
8
6
4
2
0
-2
-4
-6
-8
Energy (eV)
X
Γ
Z
states/eV/cell

Total and partial (atomic) densities of states in MnO. Only spin ↑ states are represented.

(12c)

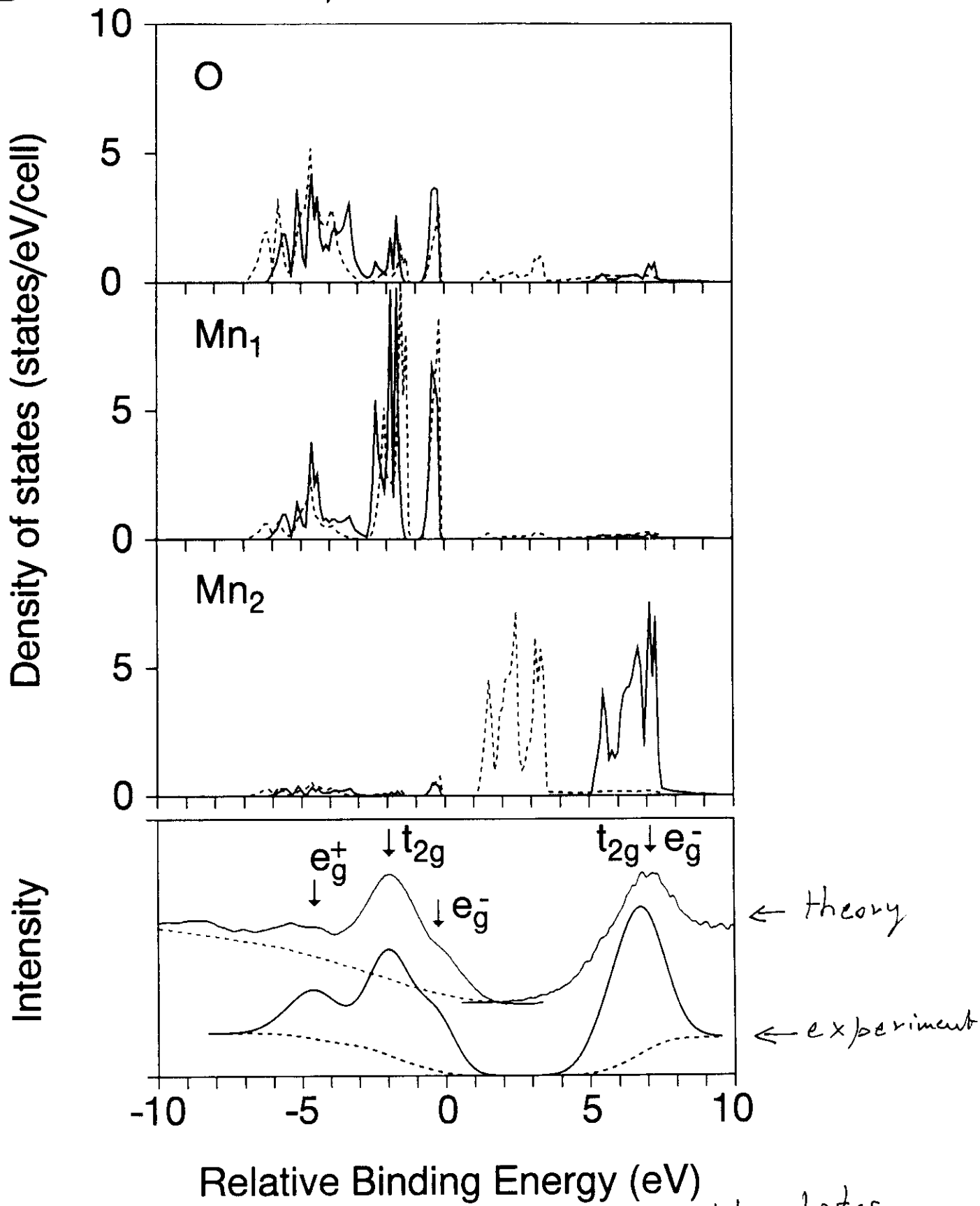

E<0 : occupied states ; E>0 : empty states

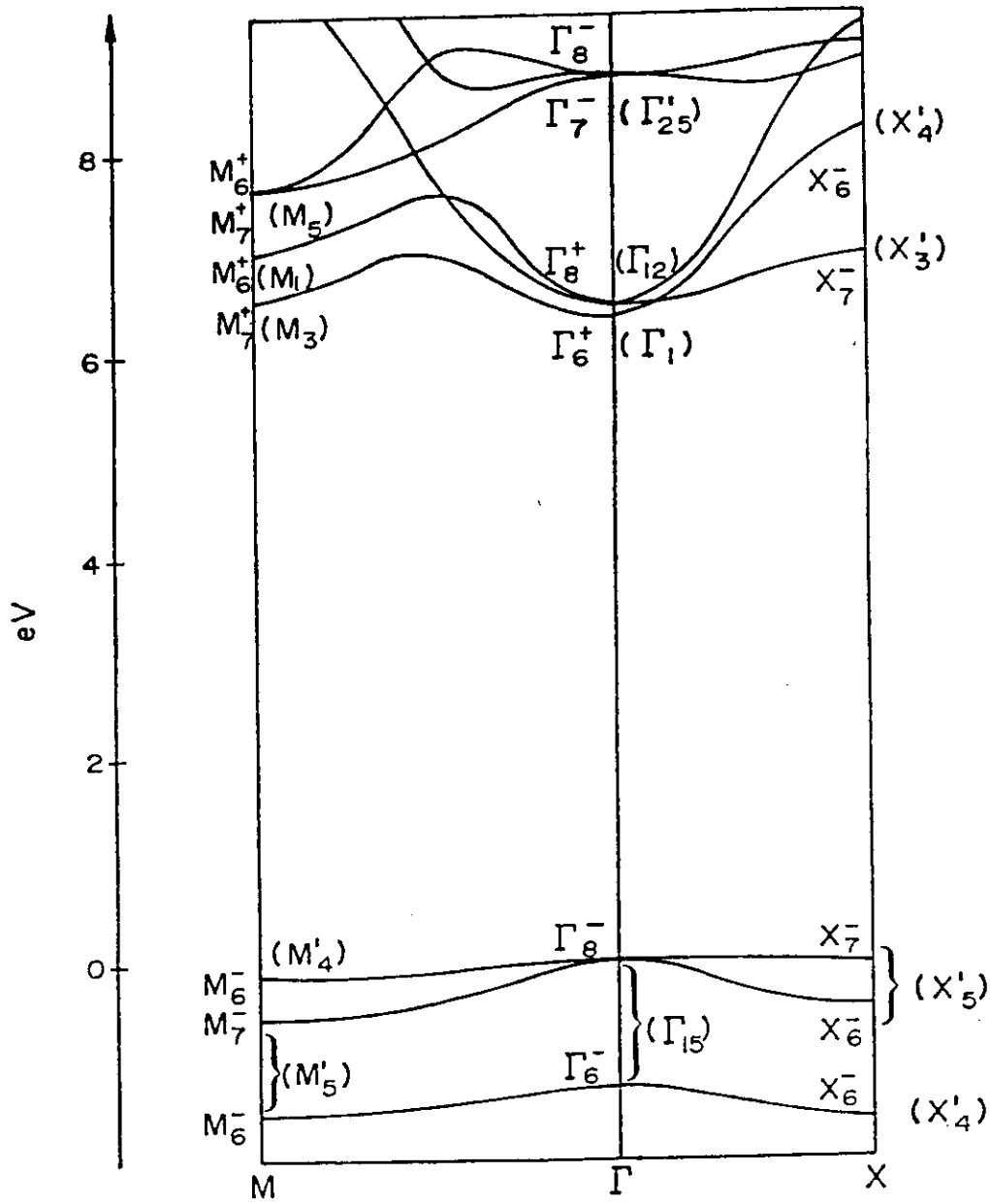

Energy bands for CsI. The notations appropriate to double group representations are used. The notations appropriate to simple group representations are given in parentheses.

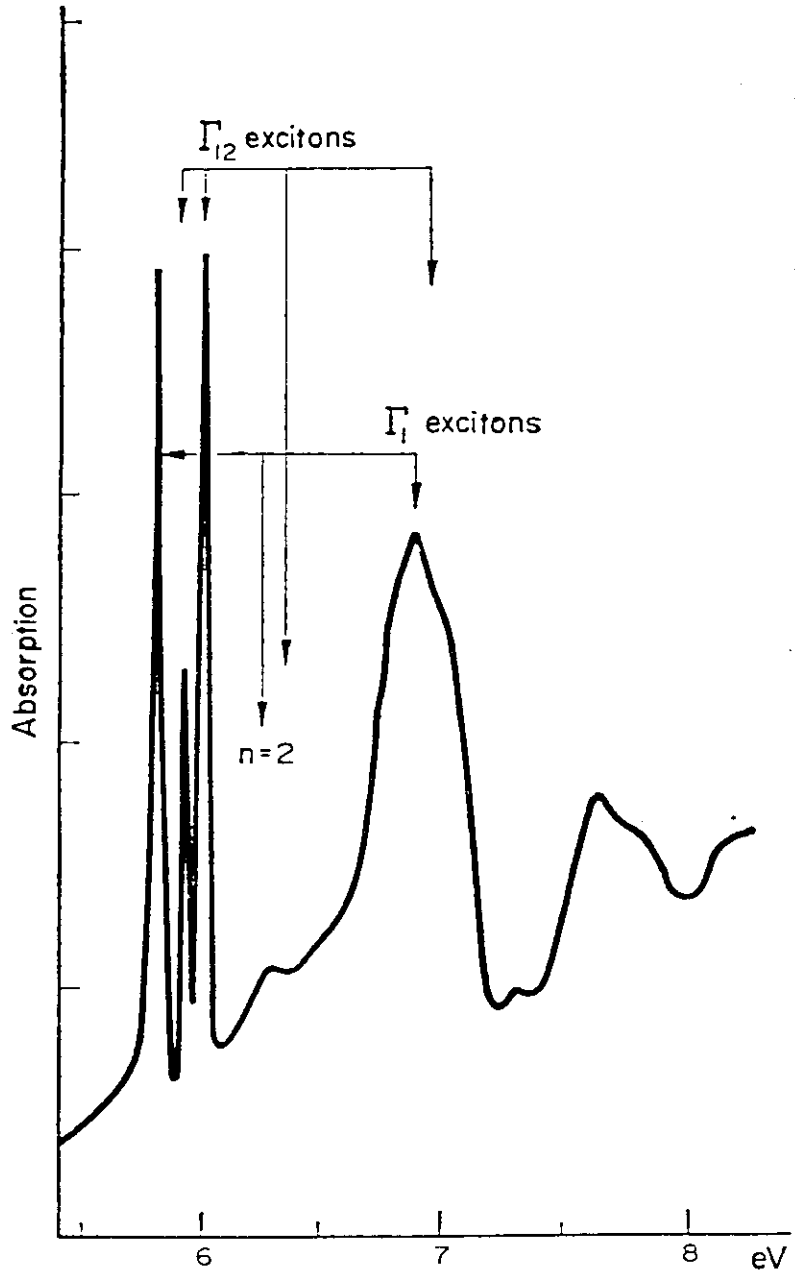

Absorption spectrum at 10K of thin CsI film. (After Teegarden and Baldini) The interpretation of exciton peaks is due to Onodera .

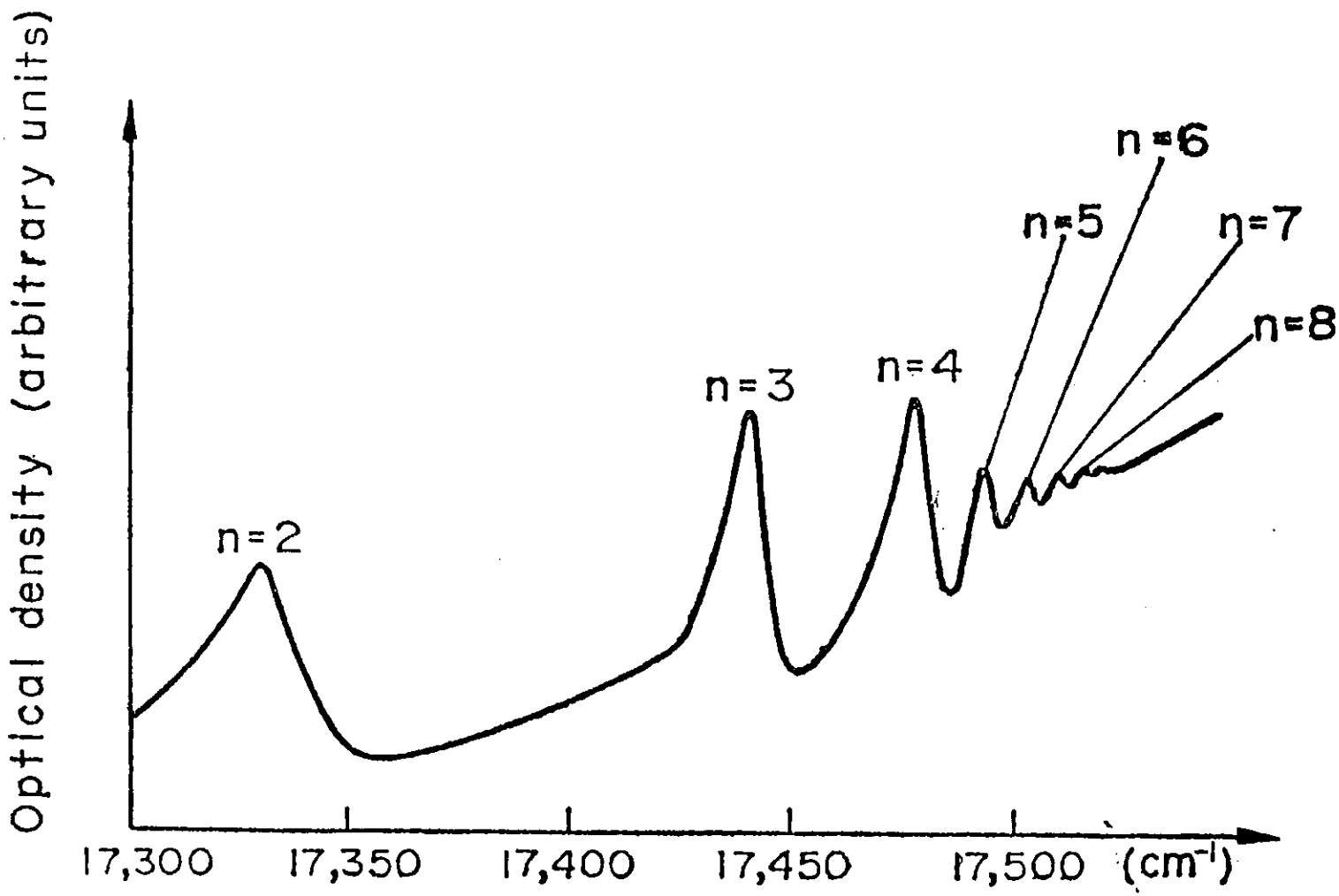

Optical density for the yellow exciton series of Cu_2O at 4.2K.

1. Radiation field in vacuum

- choice of gauge for scalar and vector potentials

$$\begin{cases} \varphi(\vec{r},t) = 0 \\ \vec{\nabla}\cdot\vec{A}(\vec{r},t) = 0 \end{cases}$$

- vector potential for monochromatic radiation

$$\vec{A}(\omega;\vec{r},t) = A_0(\omega)\,\vec{\eta}\left[e^{i(\vec{k}\cdot\vec{r}-\omega t+\delta_\omega)} + c.c.\right]$$

where $\omega = |\vec{k}|\,c$ and $\vec{\eta}\cdot\vec{k} = 0$

$|\vec{\eta}| = 1$ $\quad\vec{\eta}$ = vector of polarization

- Electric and magnetic fields

$$\begin{cases} \vec{E}(\omega;\vec{r},t) = -2\omega A_0(\omega)\,\vec{\eta}\,\sin(\vec{k}\cdot\vec{r}-\omega t+\delta_\omega) \\ \vec{E}\parallel\vec{\eta} \end{cases}$$

$$\begin{cases} \vec{B}(\omega;\vec{r},t) = -2A_0(\omega)\,\vec{k}\times\vec{\eta}\,\sin(\vec{k}\cdot\vec{r}-\omega t+\delta_\omega) \\ \vec{B}\perp k \;;\; \vec{B}\perp\vec{\eta} \end{cases}$$

2. Coupling to quantum systems

- One particle with mass m and charge q

$$h_0 = \frac{p^2}{2m} + V(\vec{r}, \vec{v})$$

$$\left\{ \begin{array}{l} \vec{p} \to \vec{p} - \frac{q}{c}\vec{A}(\omega; \vec{r}, t) \\ h_0 \to h \end{array} \right\} \text{ in presence of radiation field}$$

$$h = h_0 - \frac{q}{mc}\vec{p}\cdot\vec{A}(\omega; r, t)$$

where second order terms in A have been neglected (low radiation intensity

- N particles with masses m_i and charges q_i

$$H_0 = \sum_{i=1}^{N} \frac{p_i^2}{2m_i} + U$$

$$H = H_0 + \sum_{i=1}^{N} - \frac{q_i}{m_i c}\vec{p}_i\cdot\vec{A}(\omega; \vec{r}_i, t)$$

- Coupling operator to be used in time-dependent perturbation theory

$$W = \sum_{i=1}^{N} - \frac{q_i A_0(\omega)}{m_i c}\vec{\eta}\cdot\vec{p}_i \left[e^{+i(\vec{k}\cdot\vec{r}_i - \omega t + \delta_\omega)} + c.c \right]$$

3. Dipole approximation

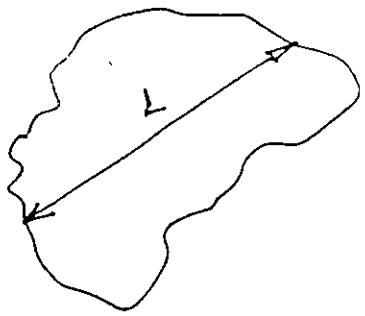

L = linear dimension of quantum system (~ 10 Å)

If $k L \ll 1$ the coupling operator can be approximated as:

$$W \simeq - \frac{A_0(\omega)}{c} \left[e^{-i(\omega t - \delta_\omega)} + c.c. \right] \sum_{i=1}^{N} \frac{q_i}{m_i} \vec{\eta} \cdot \vec{p}_i$$

and its matrix element between initial state $|\psi_0\rangle$ and final state $|\psi_f\rangle$ becomes

$$\langle \psi_f | W | \psi_0 \rangle = - \frac{A_0(\omega)}{c} \left[e^{-i(\omega t - \delta_\omega)} + c.c \right] \sum_{i=1}^{N} \frac{q_i \vec{\eta}}{i\hbar} (E_0 - E_f) \langle \psi_f | \vec{r}_i | \psi_0 \rangle$$

$$= \frac{i A_0(\omega)}{\hbar c} \left[e^{-i(\omega t - \delta_\omega)} + c.c. \right] (E_0 - E_f) \vec{\eta} \langle \psi_f | \sum_{i=1}^{N} q_i \vec{r}_i | \psi_0 \rangle$$

where $\sum_{i=1}^{N} q_i \vec{r}_i$ is the electric dipole operator of the system.

In the above derivation, use has been made of the relationship

$$\vec{p}_i = (-i\hbar)^{-1} [\vec{r}_i, H_0] .$$

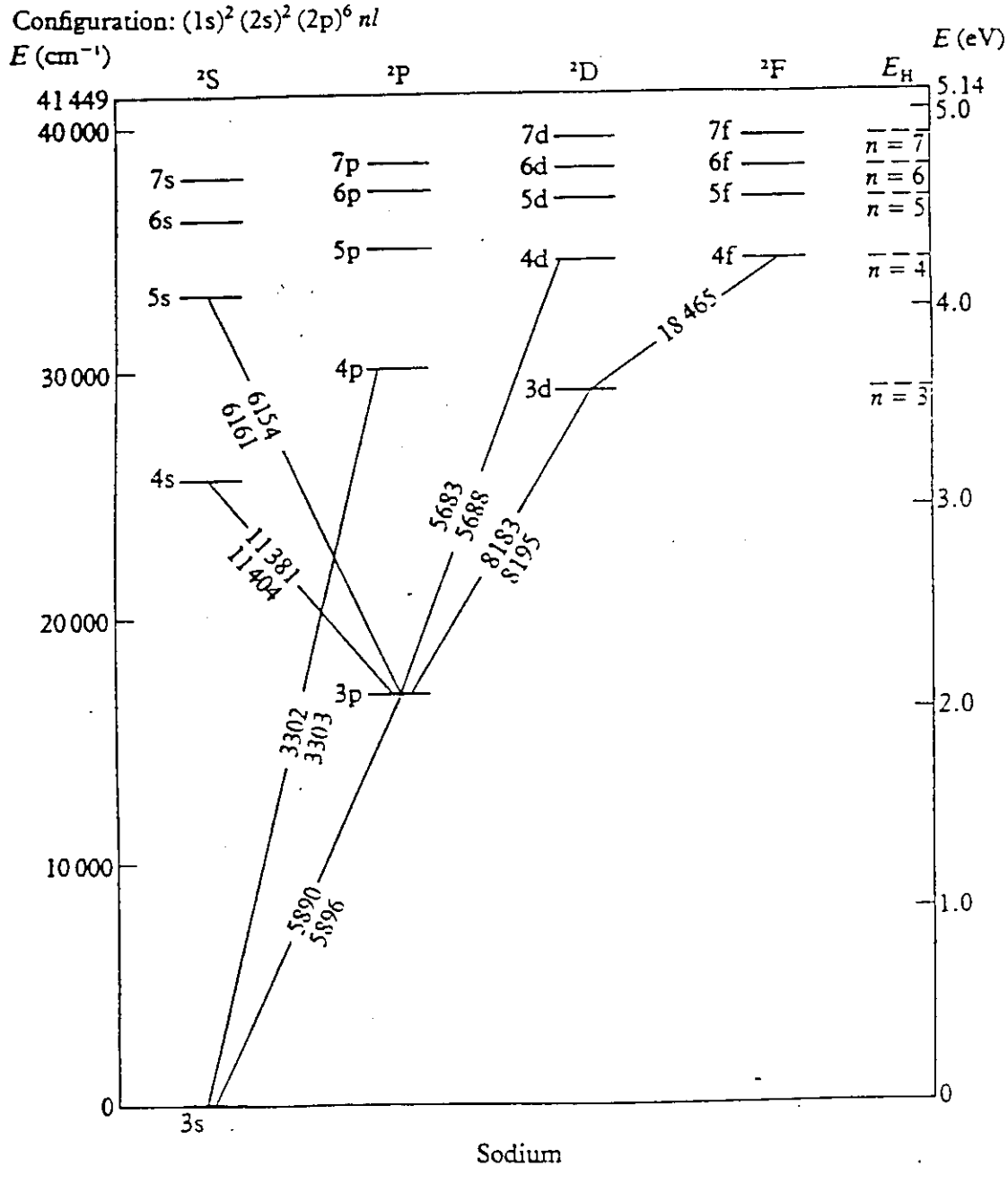

Allowed optical transitions in atomic sodium. Notice selection rule $\Delta \ell = \pm 1$, ℓ = angular momentum.

Energy bands of Ge close to the fundamental gap.

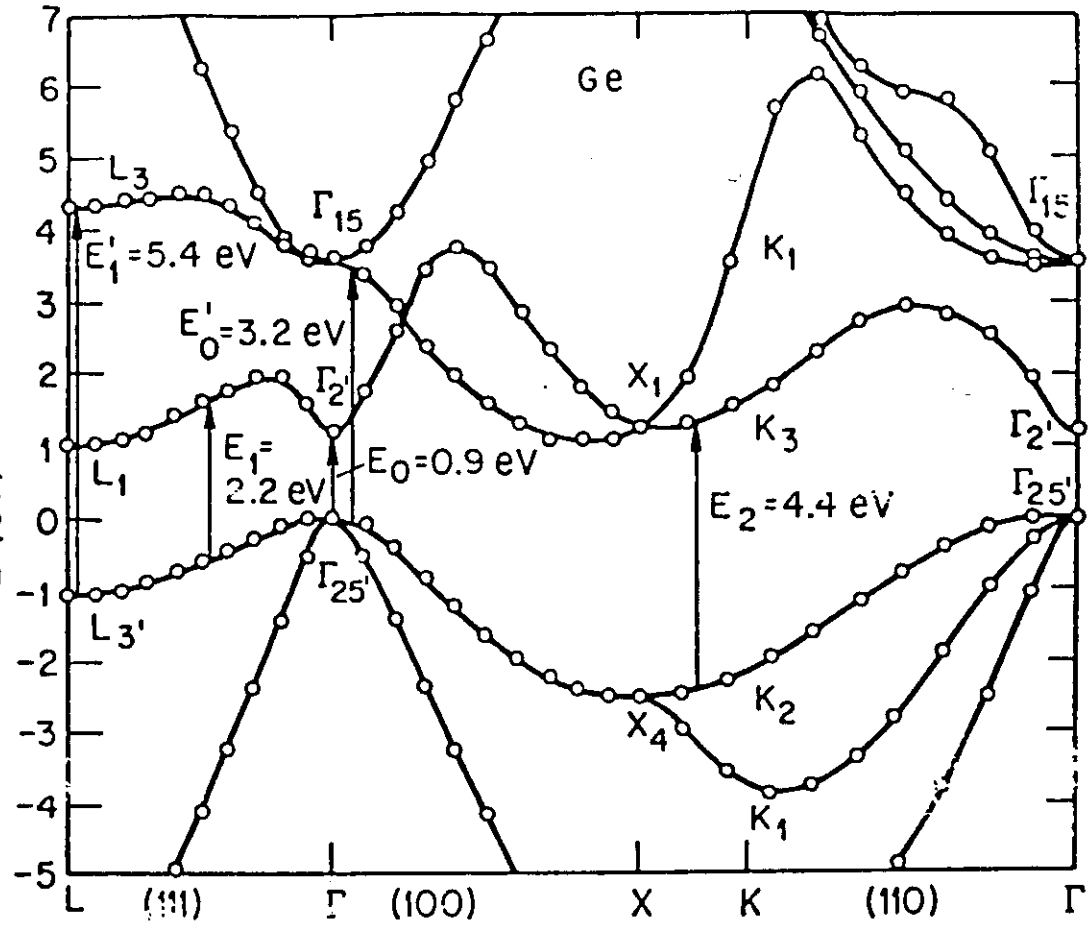

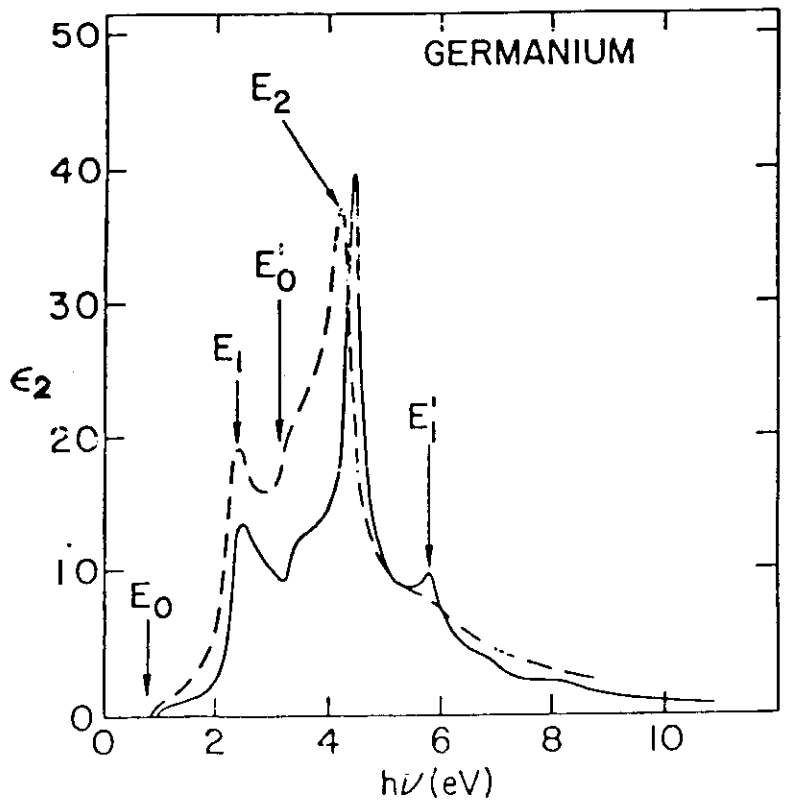

Energy dependence of the imaginary part of the dielectric function of Ge. Experimental data (solid line) from H. R. Philipp and H. Ehrenreich, Phys. Rev. 129, 1550 (1963), calculated spectrum (broken line)

Neglect of photon momentum in the dipole approximation, i.e. vertical electronic transitions for low-energy photons.

SPECTRAL REGIONS FOR USING SYNCHROTRON RADIATION

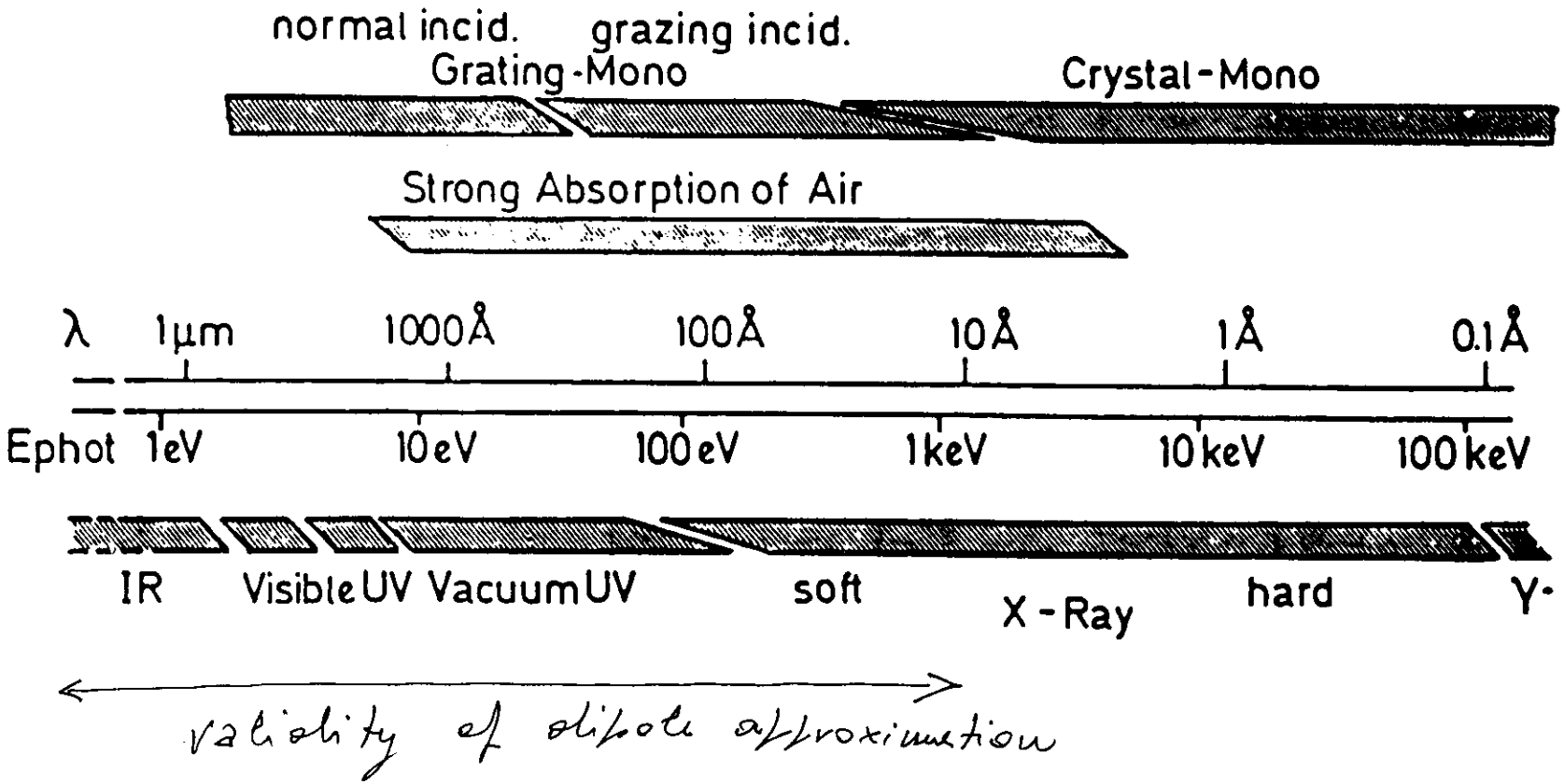

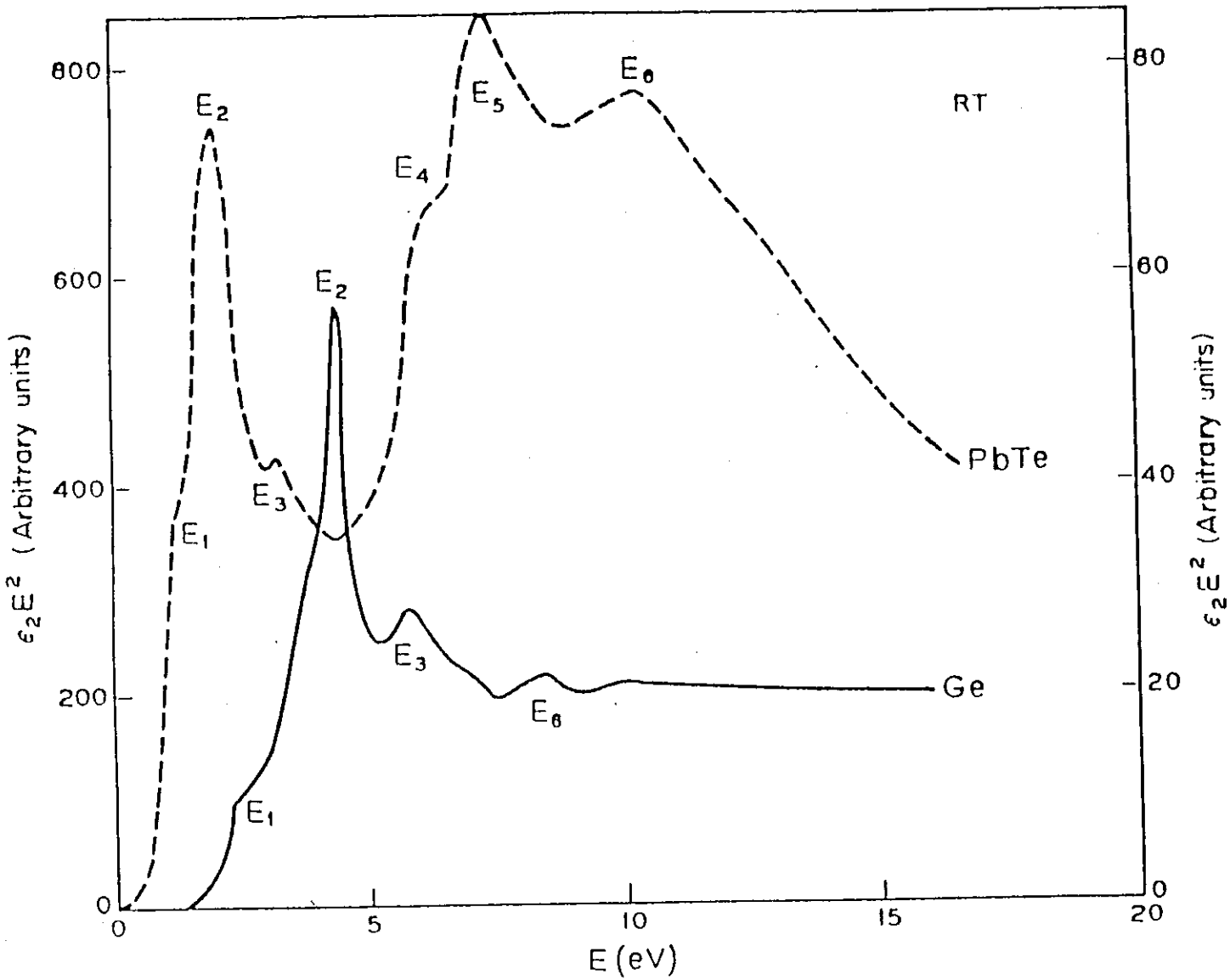

The density of states function $\epsilon_2 E^2$ for Ge and PbTe derived from normal incidence reflectance data.

Both materials are cubic. No optical anisotropy is observed.

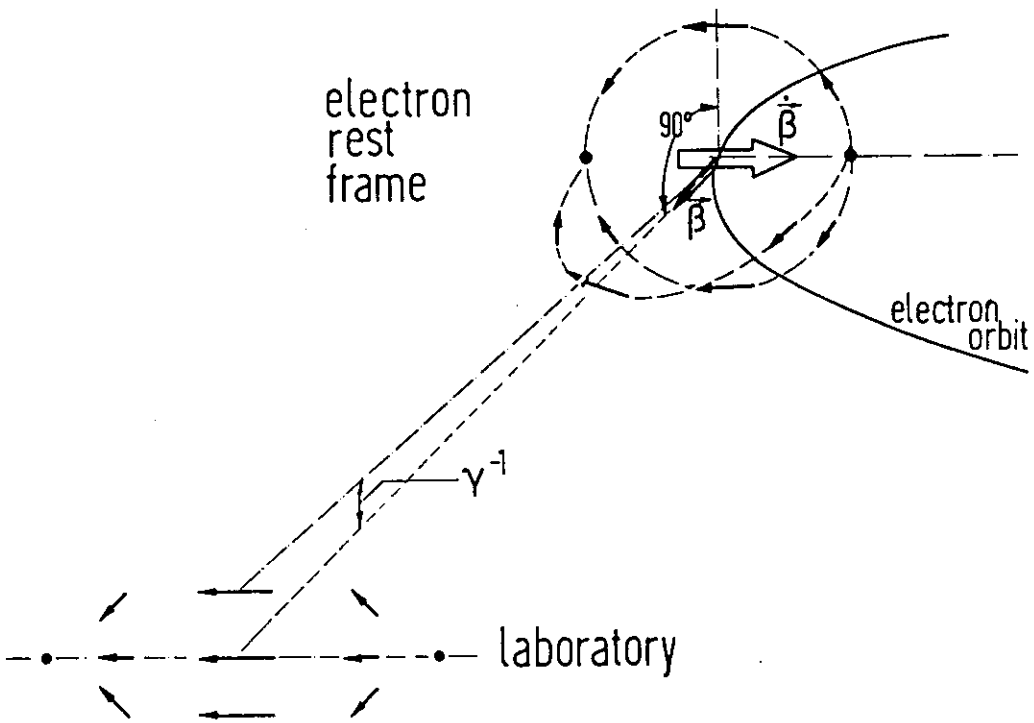

Non-relativistic dipole radiation pattern and its appearance after the relativistic angle transformation. Arrows indicate direction and magnitude of the electric vector

Polarization of synchrotron light

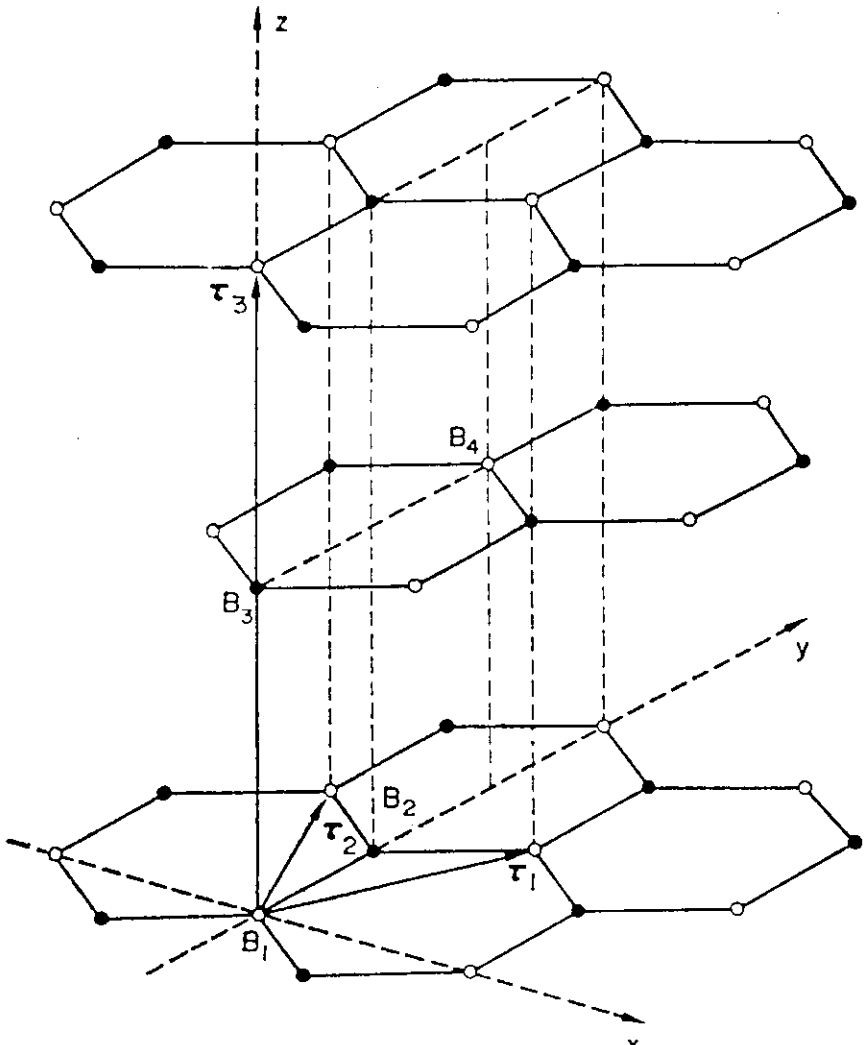

Crystallographic structure of graphite. Strong sp^2 covalent bond in the planes. Weak interatomic interactions between the planes.

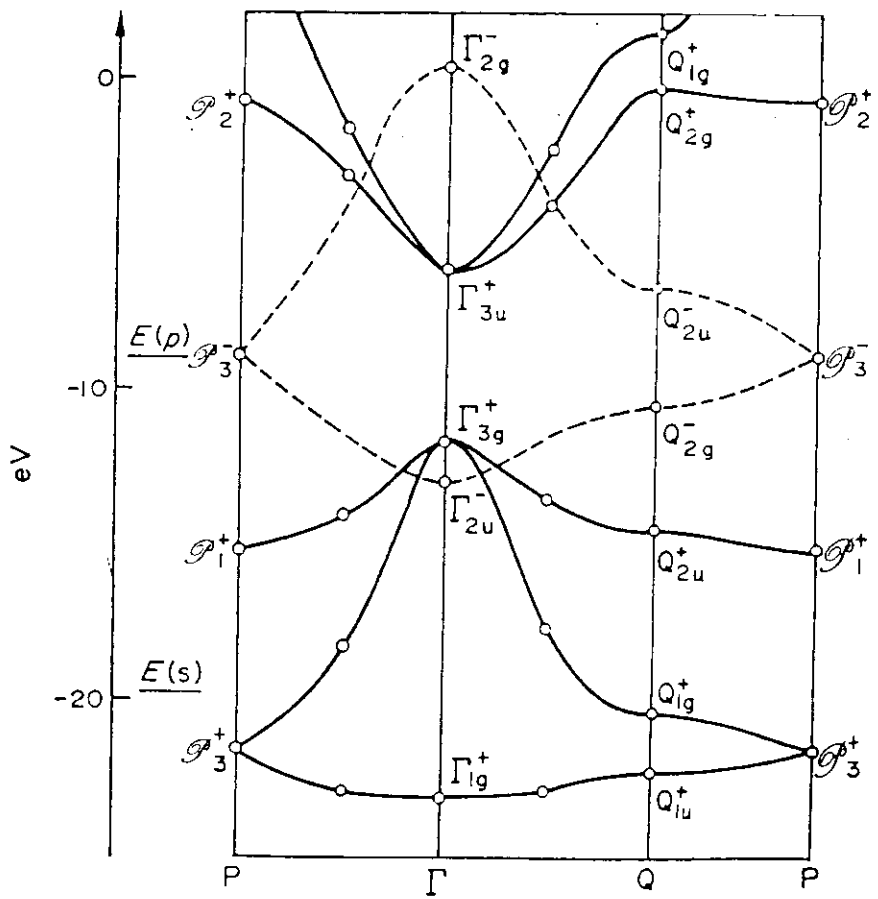

Energy bands for two-dimensional graphite. Bands even (odd) with respect to the σ_h reflection are denoted by continuous (broken) lines. The energies of the valence states of carbon atom are also shown.

Example of polarization effect.

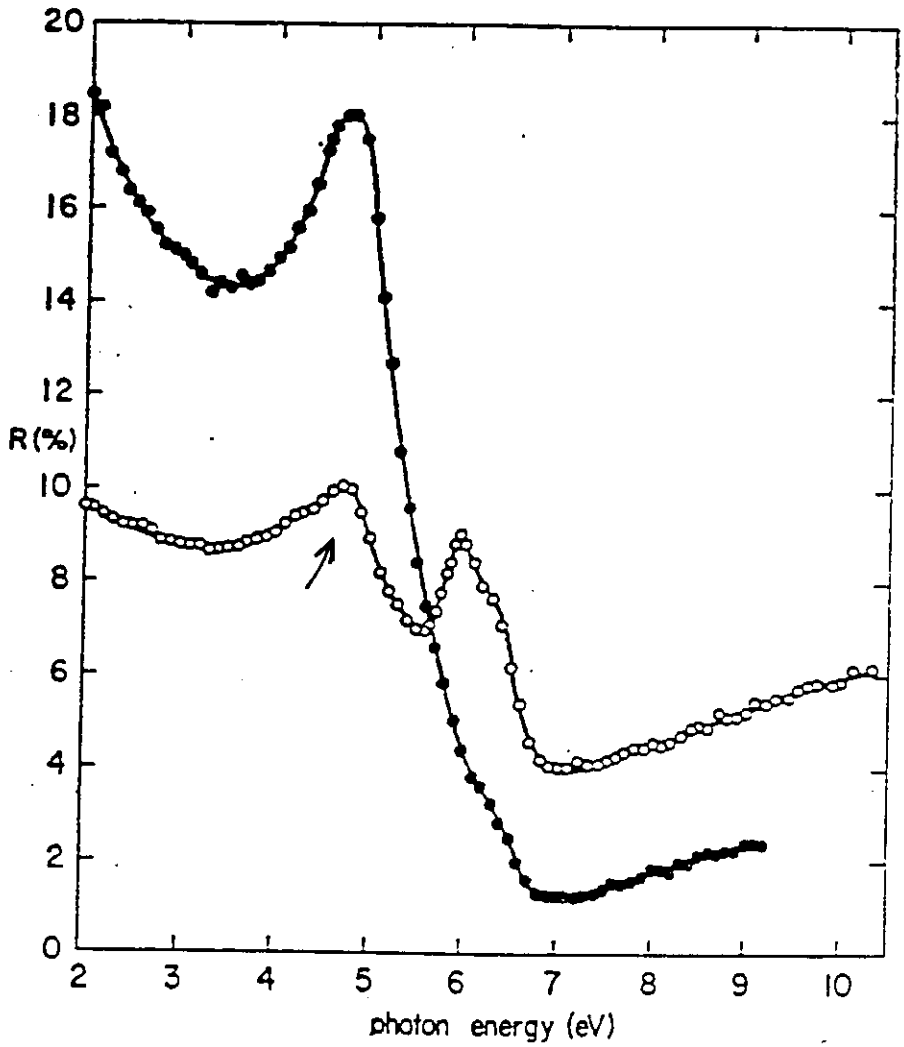

Reflectivity of polished pyrolytic graphite for (●) $E \perp c$ and (○) $E \| c$ under near-normal incidence.

The arrow indicates a residue of the $E \perp c$ spectrum. Should not be there for perfect normal incidence and perfect sample.

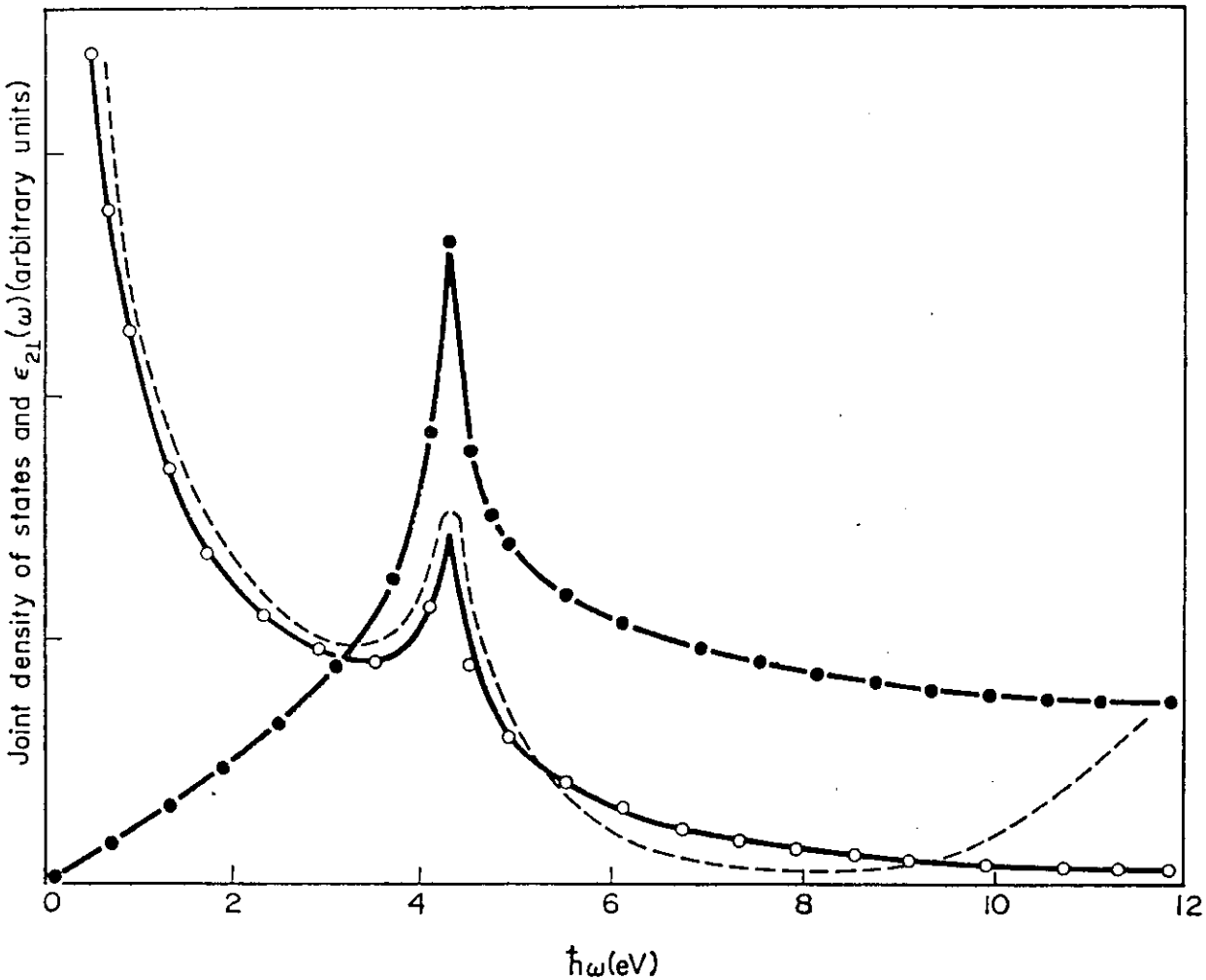

Joint density of states (solid circles) and imaginary part of the dielectric constant (open circles) computed from the π bands of two-dimensional graphite. The experimental dielectric function of Taft and Philipp is also given.

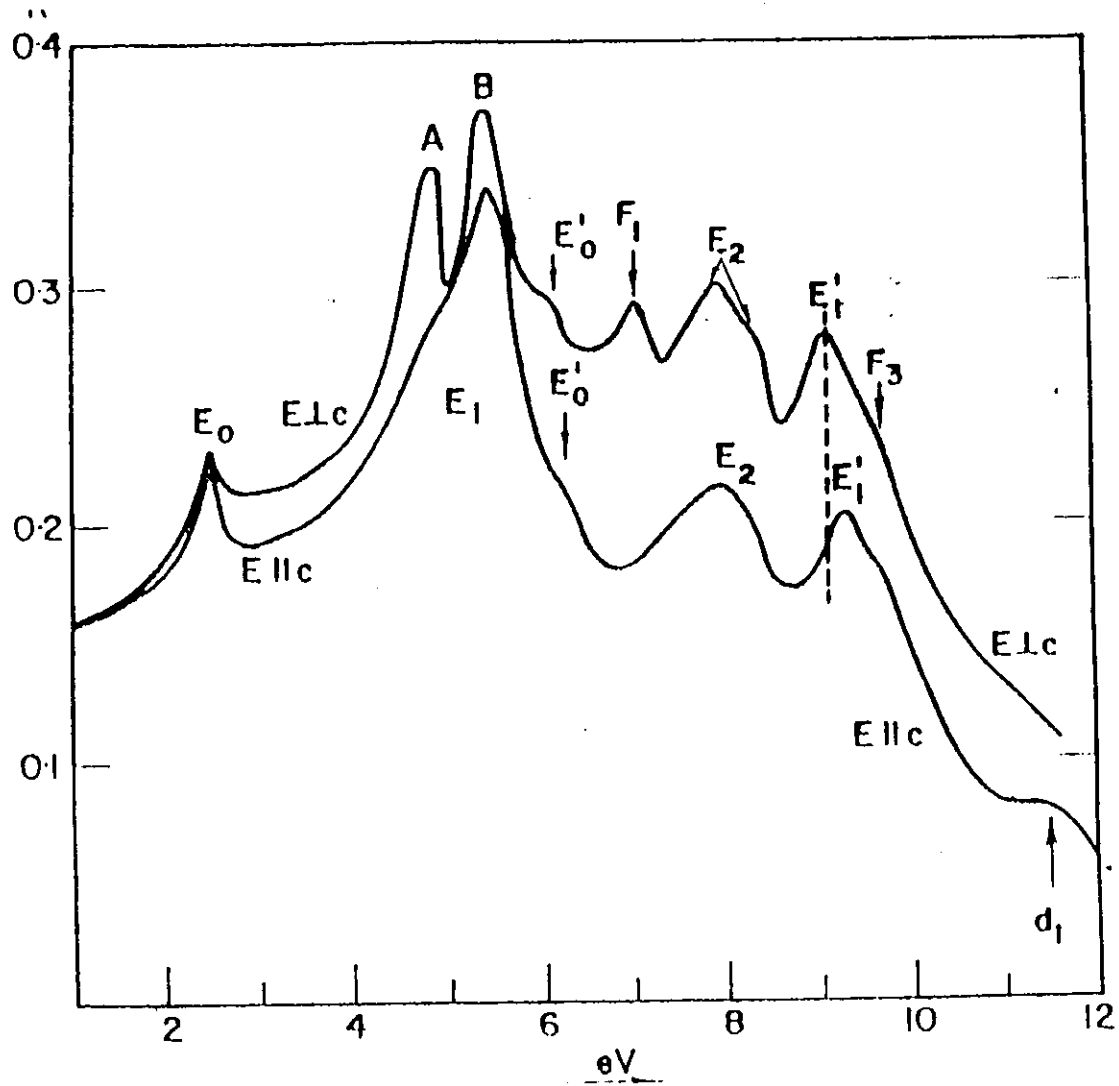

Room temperature reflectivity of hexagonal CdS for $E \perp c$ and $E \parallel c$ (Cardona and Harbeke).

Polarization effect for weak anisotropy.

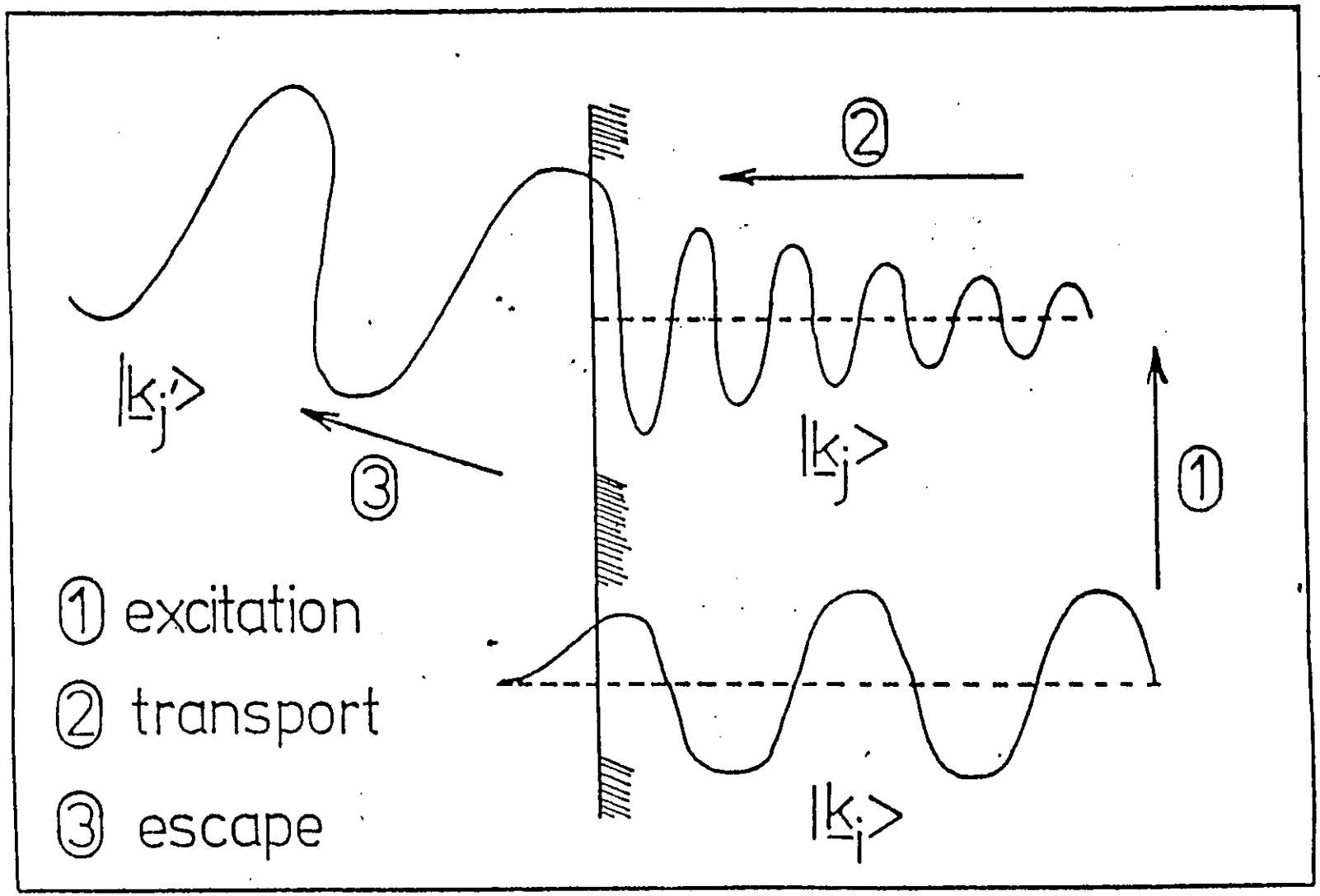

Scheme of photoemission experiment.

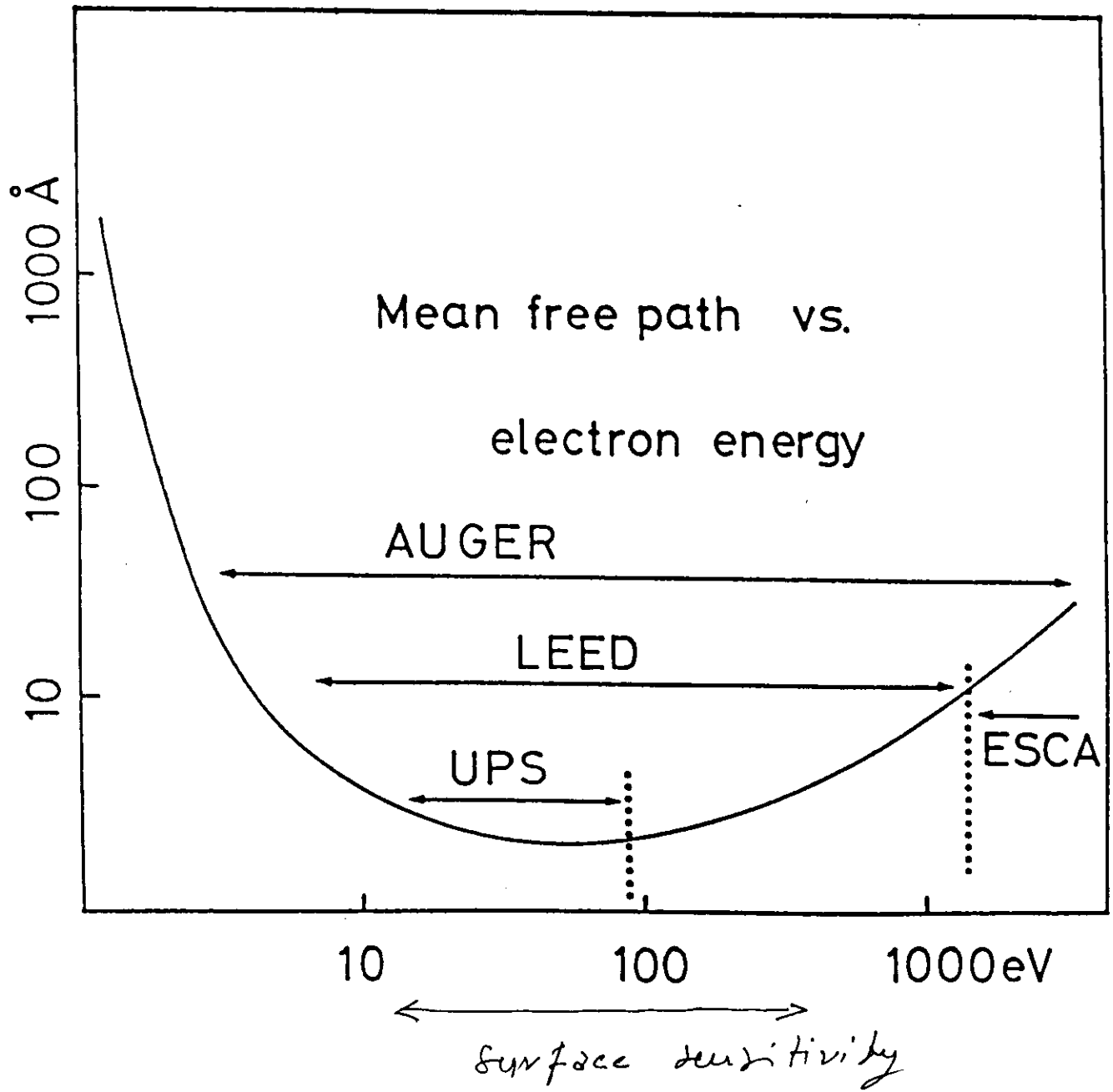
Mean free path vs.
electron energy
1000 Å
100
10
AUGER
LEED
UPS
ESCA
10
100
1000eV
surface sensitivity

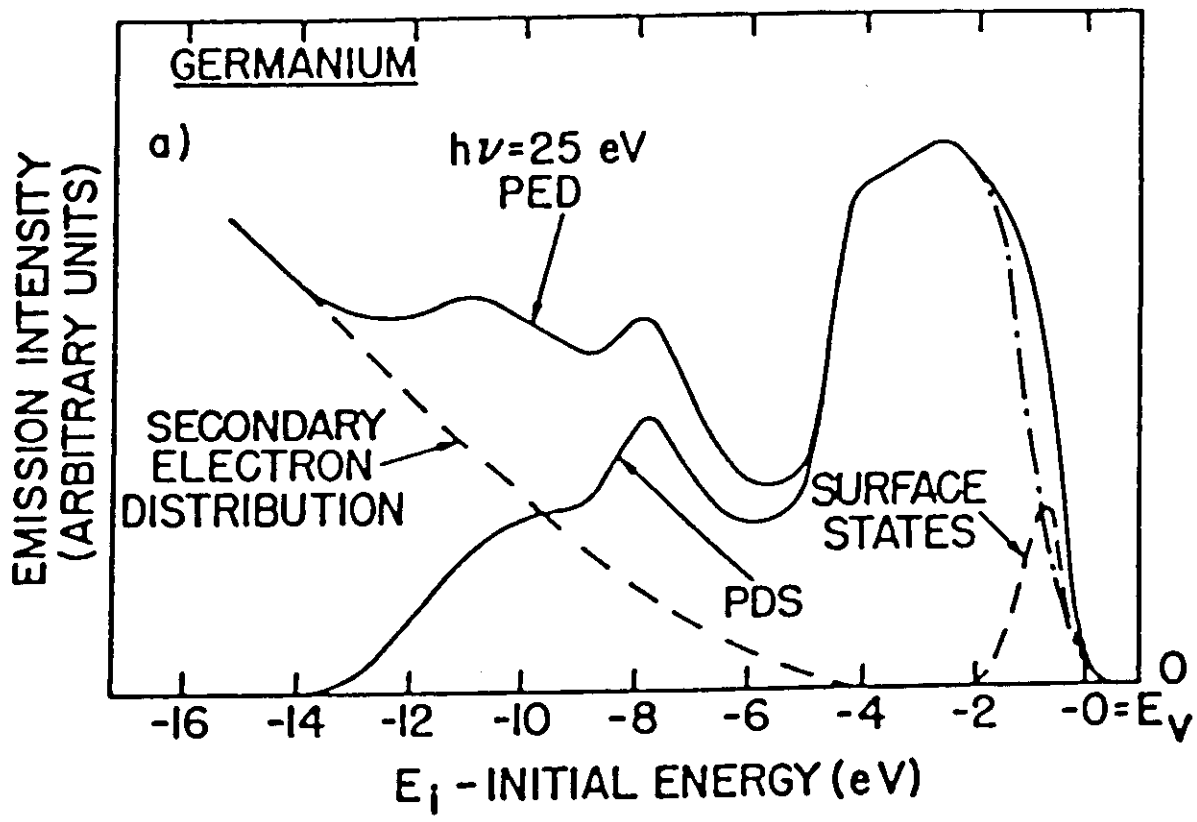

Photoemission intensity and photoemission density of states of Ge. (W. D. Grobman, D. E. Eastman, and J. L. Freeouf, Phys. Rev. 12B, 4405 (1975))

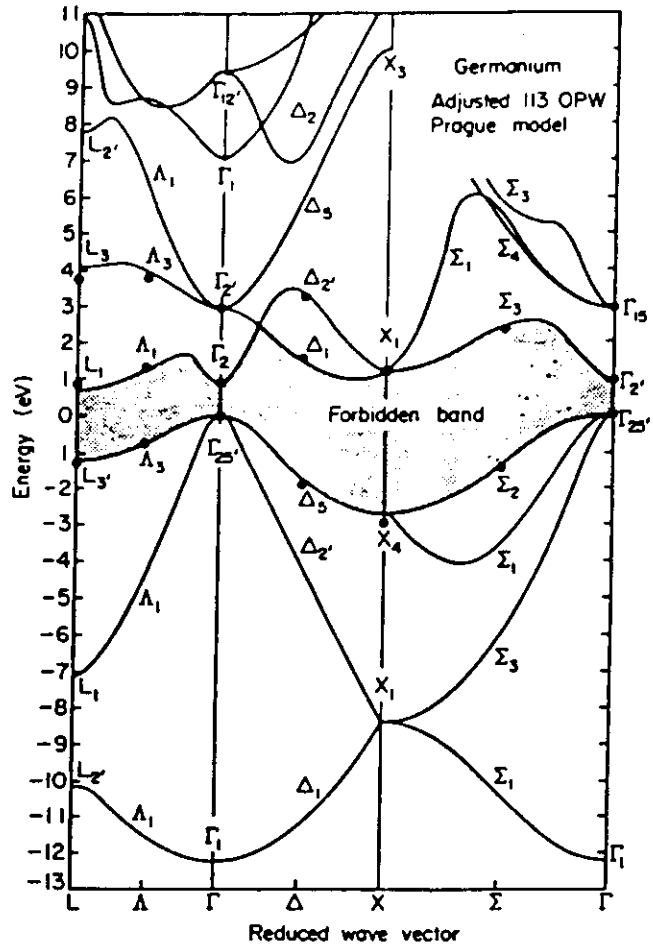

Energy band structure of germanium, with spin-orbit splitting neglected. Representative points of the pseudopotential interpolation scheme fitted to this adjusted OPW band model are indicated by the heavy dots (after Herman *et al.*, 1967a,b).

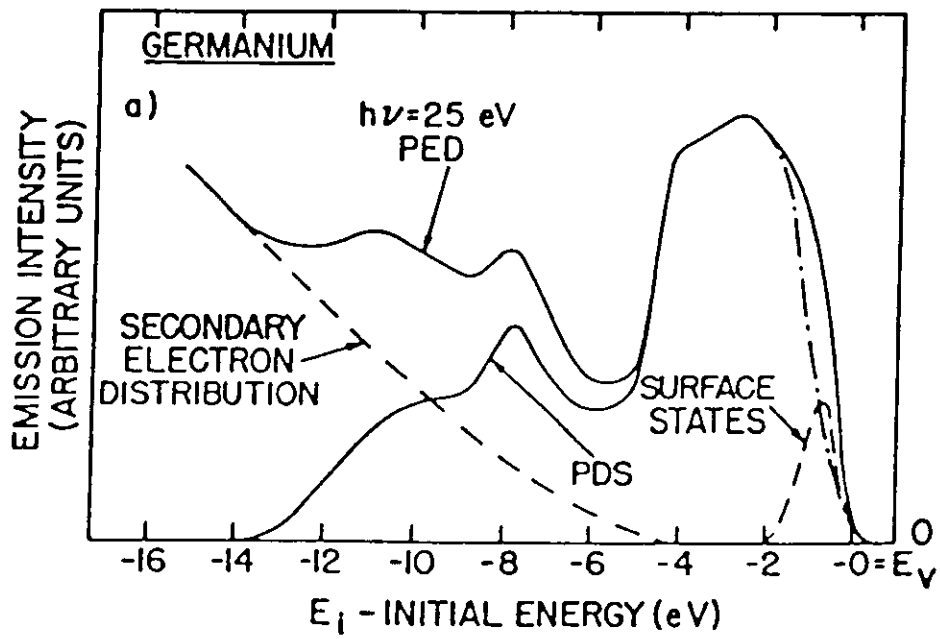

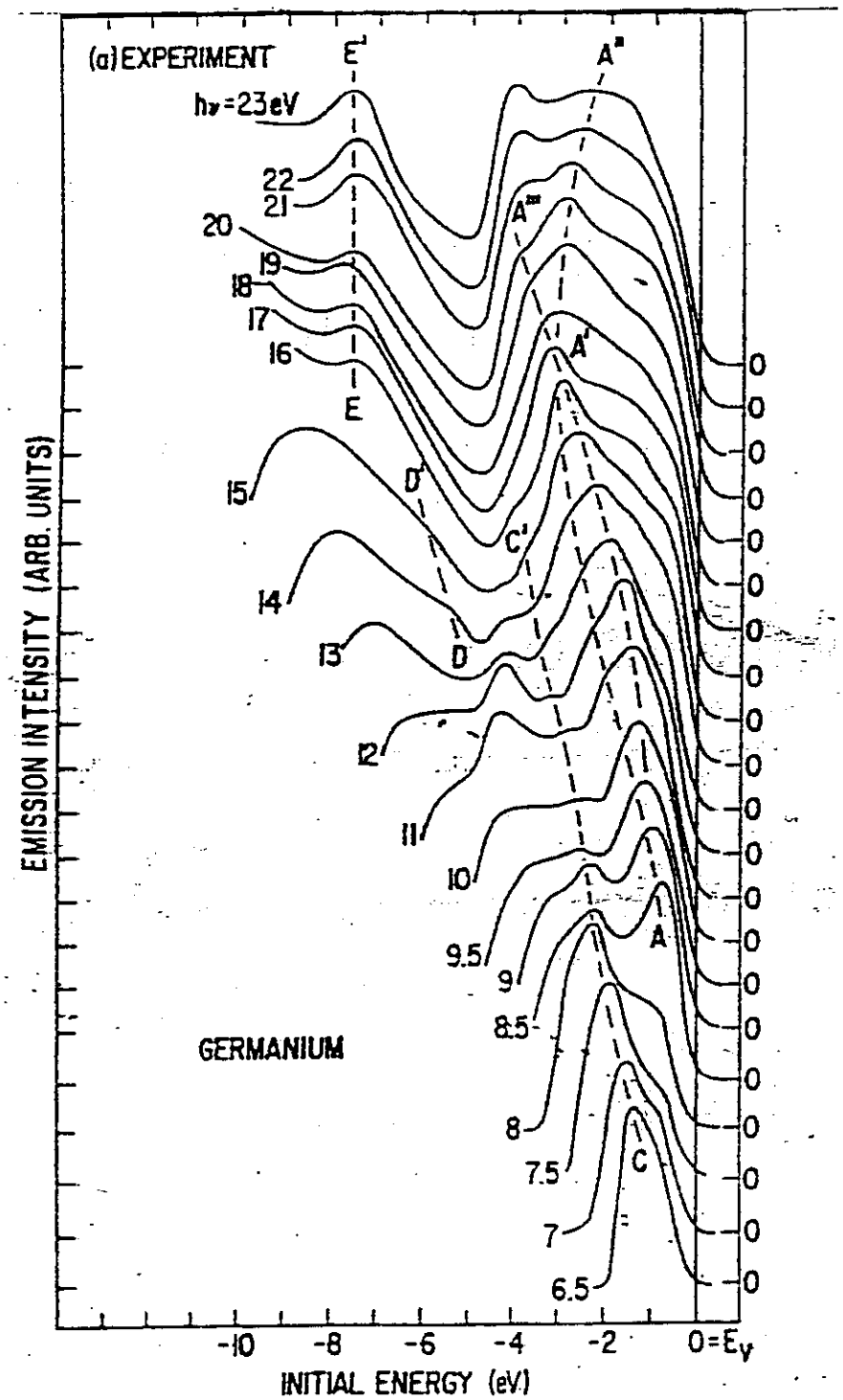

Final-state effects in low-energy UPS data in Ge.

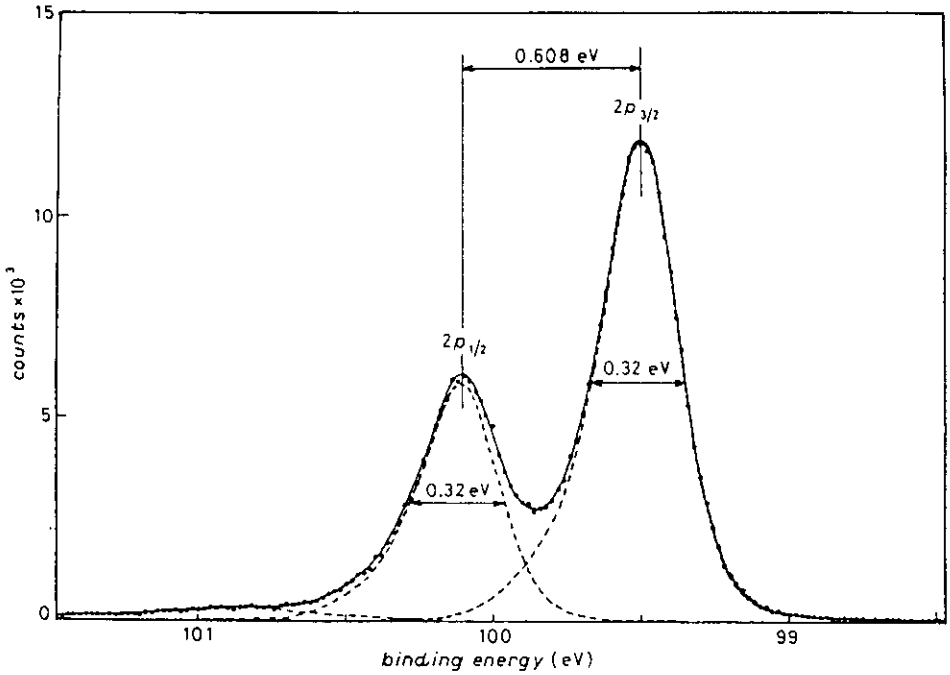

The Si2*p* core level of bulk Si measured by X-ray photoelectron spectroscopy (from ref. [9]); Si(111), $T = 300$ K, $\theta = 45°$.

Notice core spin-orbit separation.

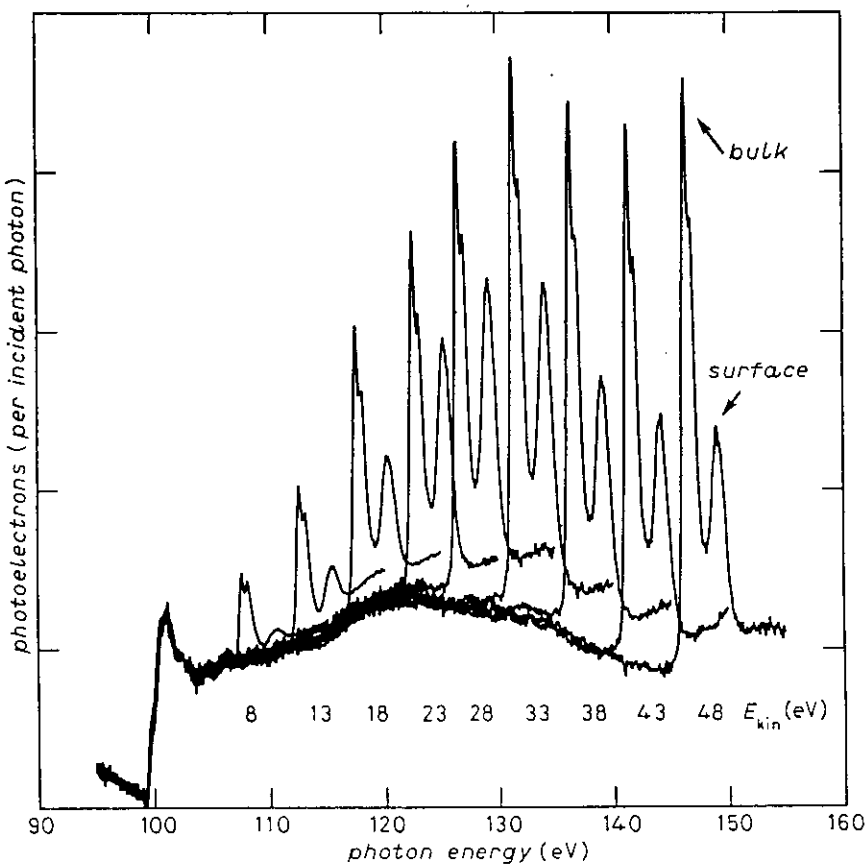

Constant-final-state spectra for oxygen on Si(100) exhibiting energy-dependent variations in the photoionization cross-section and in the escape depth. A maximum in the surface-to-bulk intensity ratio is reached at about 130 eV photon energy.

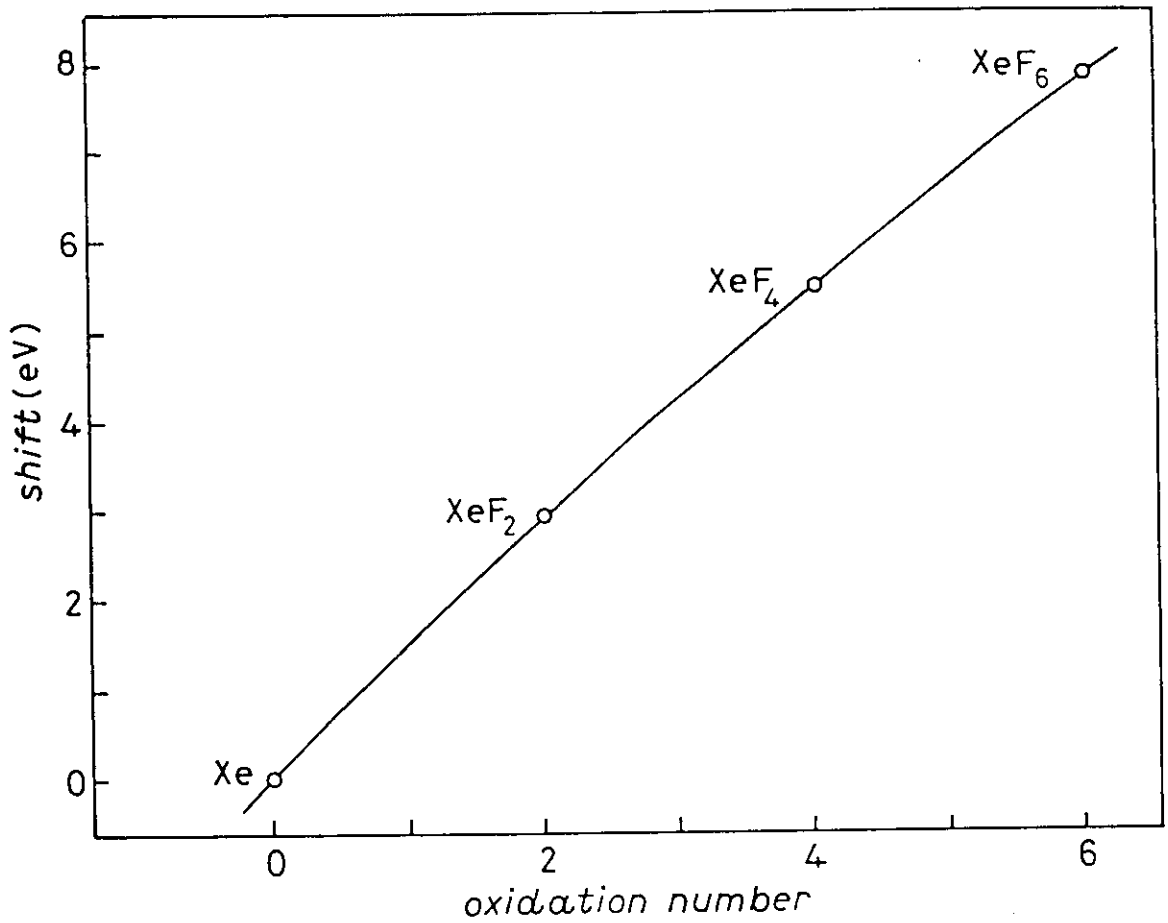

Measured binding energy shift for the xenon $3d_{5/2}$ electrons

Chemical shifts of Xe core levels when atom is embedded in different environments.

Chemical shifts increase (decrease) binding energy of core levels of positive (negative) atoms.

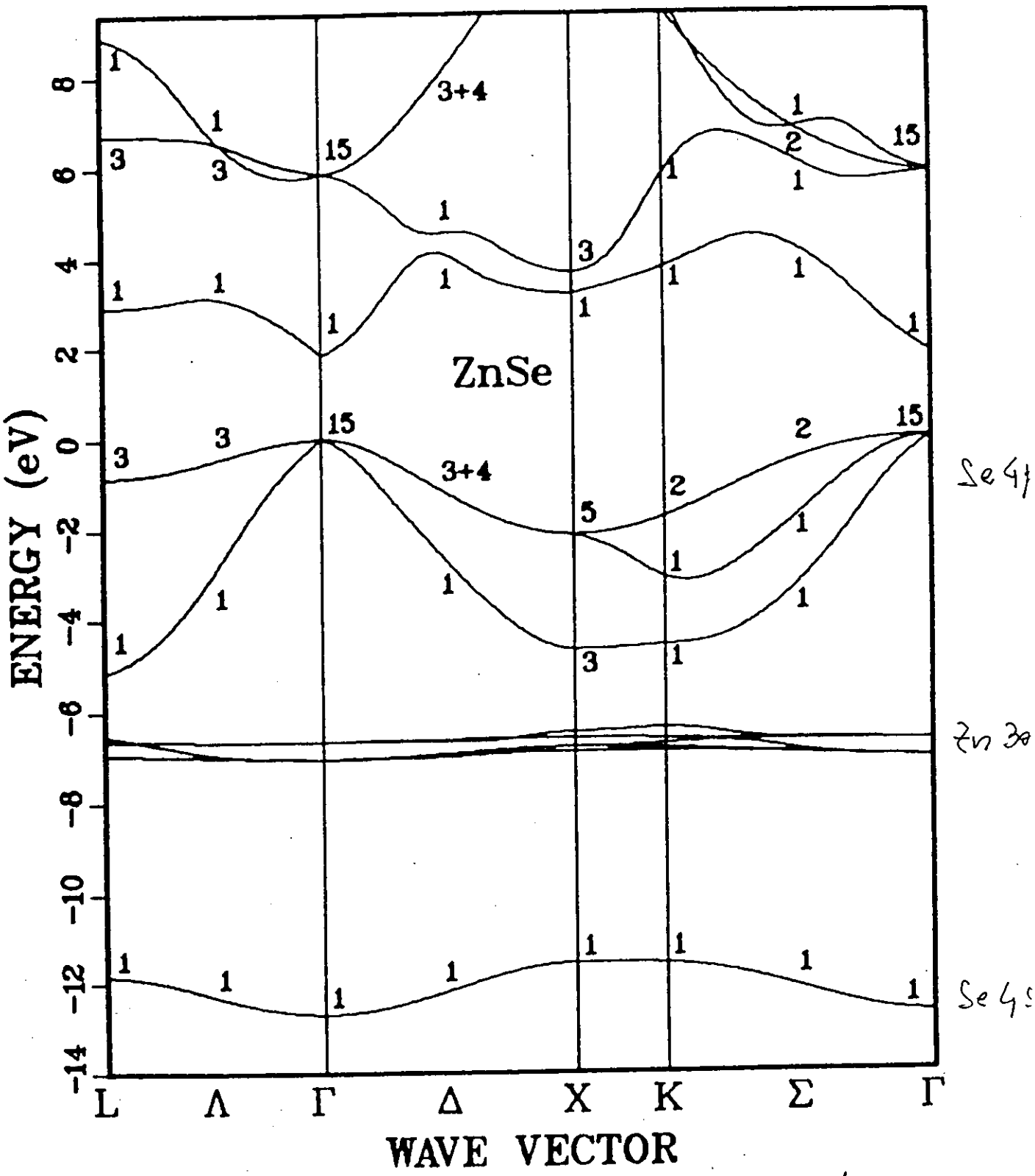

Energy - band dispersion of ZnSe close to the fundamental gap.

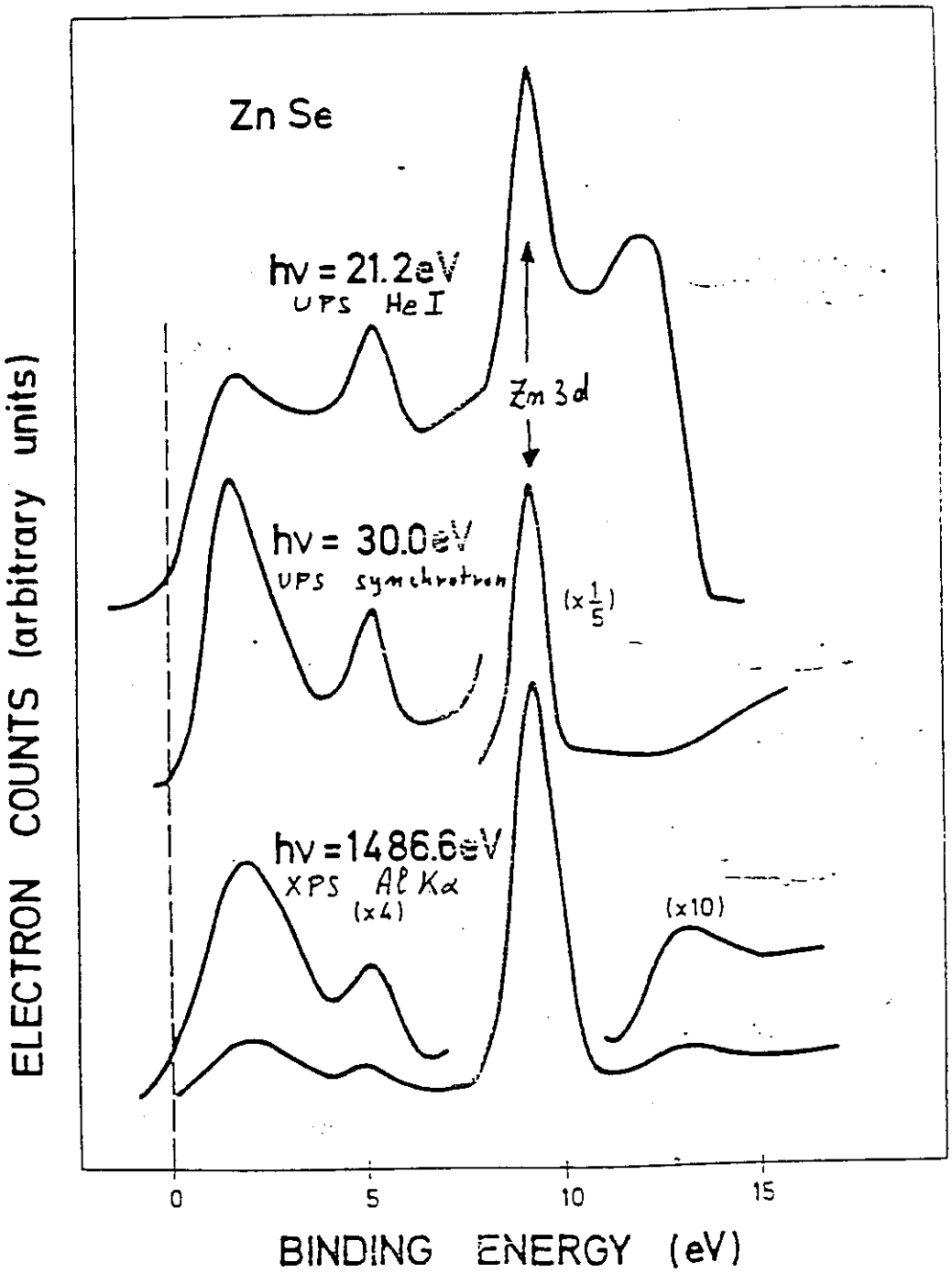

Photoemission spectra of Zn Se obtained with different photon sources. Notice sharp structure due to Zn 3d bands.

Band structure of ZnO within different approximations.
Notice the different relative position of O2p - bands and Zn 3d - bands.

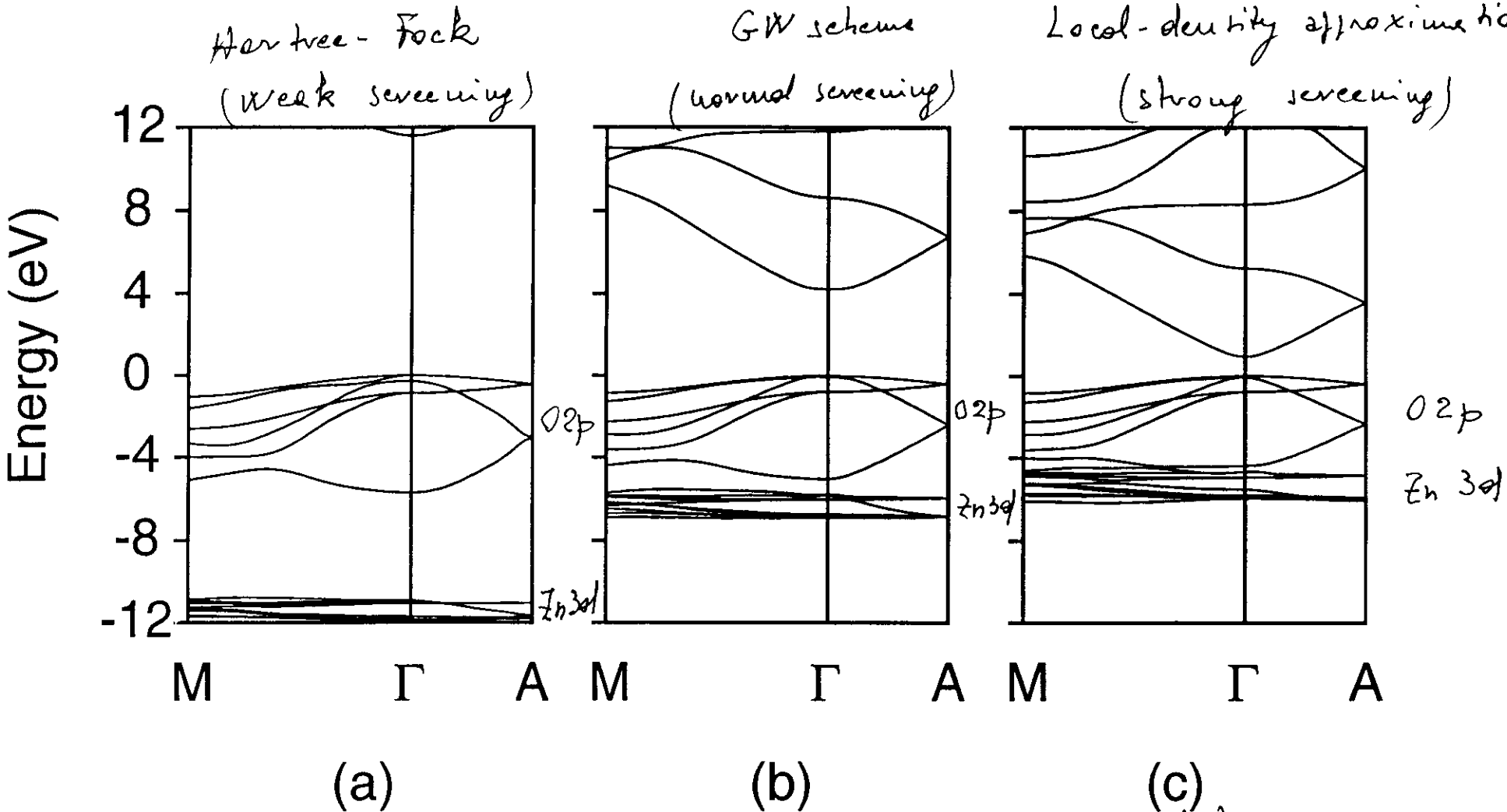

$E < 0$: occupied states ; $E > 0$ empty states.

Massidda et al, PRB, Figure 1

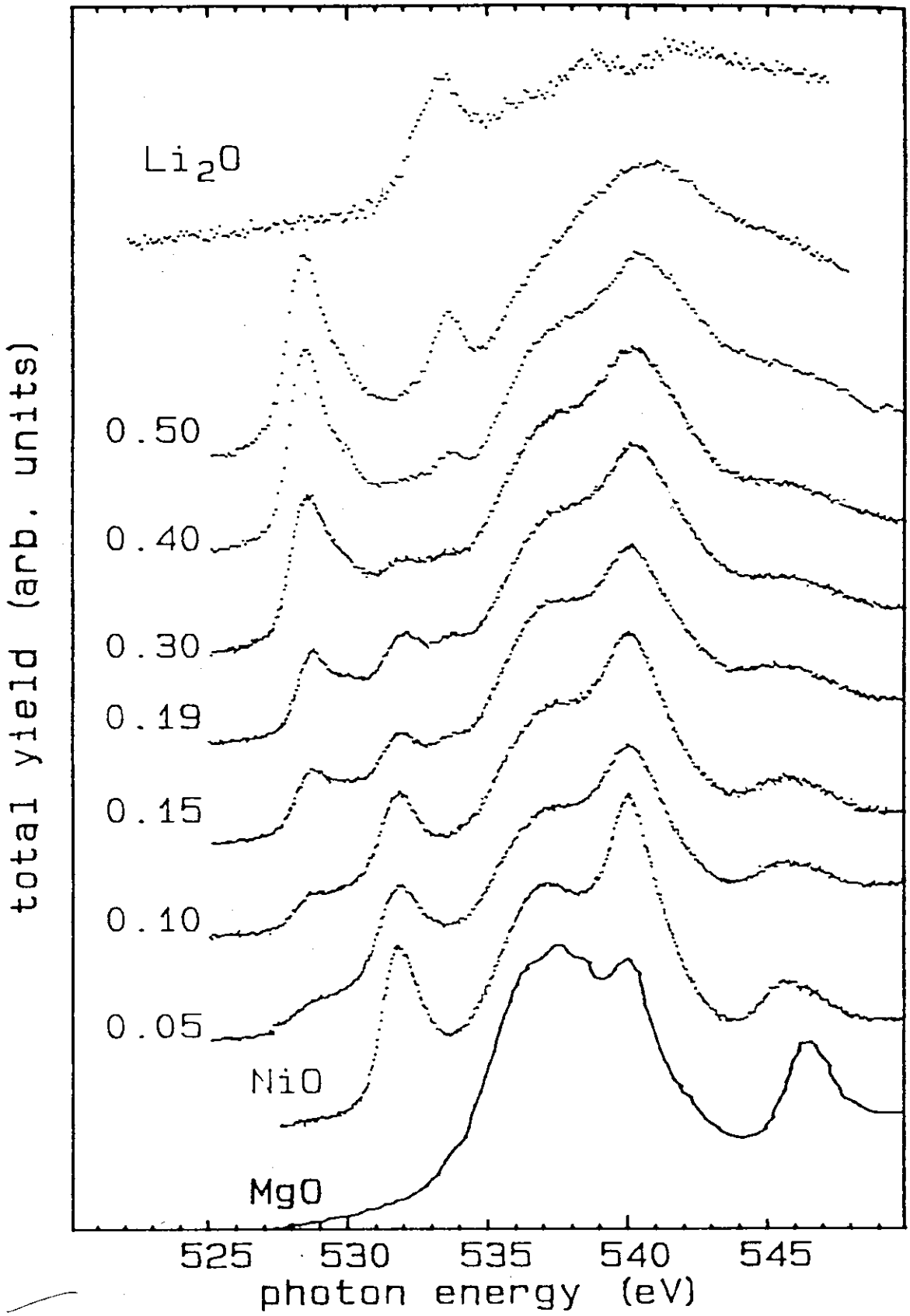

Oxygen *K*-edge absorption spectra of MgO NiO, $Li_xNi_{1-x}O$ for indicated values of x, and Li_2O.

K-edge spectra of Li-doped NiO give evidence that topmost occupied states in NiO derive also from O2p orbitals.

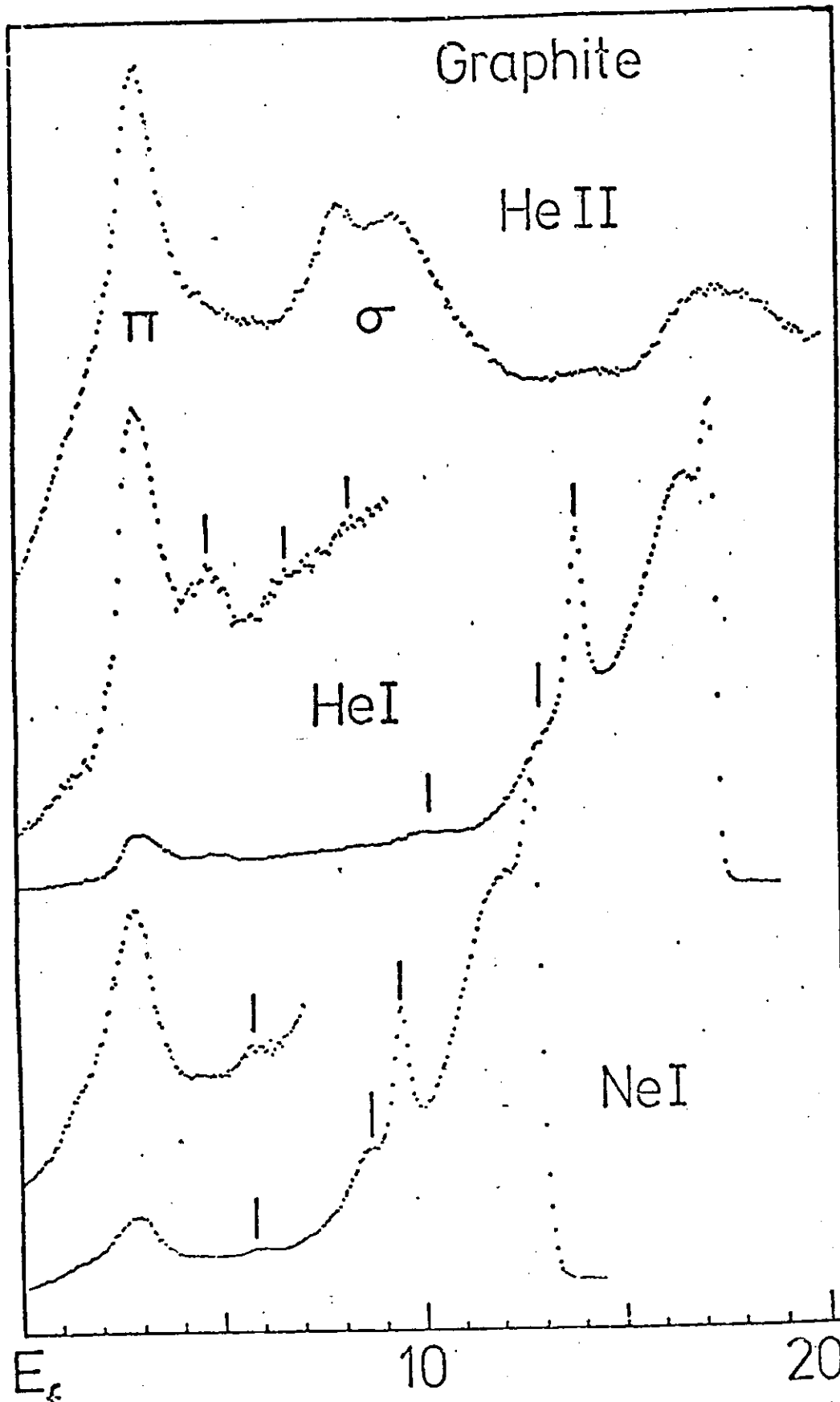

UPS spectra of graphite with different sources.

PHOTOEMISSION : SOURCES

1. UPS

5 - 100 eV

- Spectres atomiques ou moléculaires

He I	21.2 eV
He II	40.8 eV
He IIβ	48.8 eV
Ne I	16.8 eV
Ne II	26.9 eV

- Synchrotron (intensity + tunability + polarization).

2. XPS (ESCA)

$\sim 10^3$ eV

- Rayons X - Emission par atome

Mg	Kα	1253.6 eV
Al	Kα	1486.6 eV

- Synchrotron (intensity + tunability + polarization).

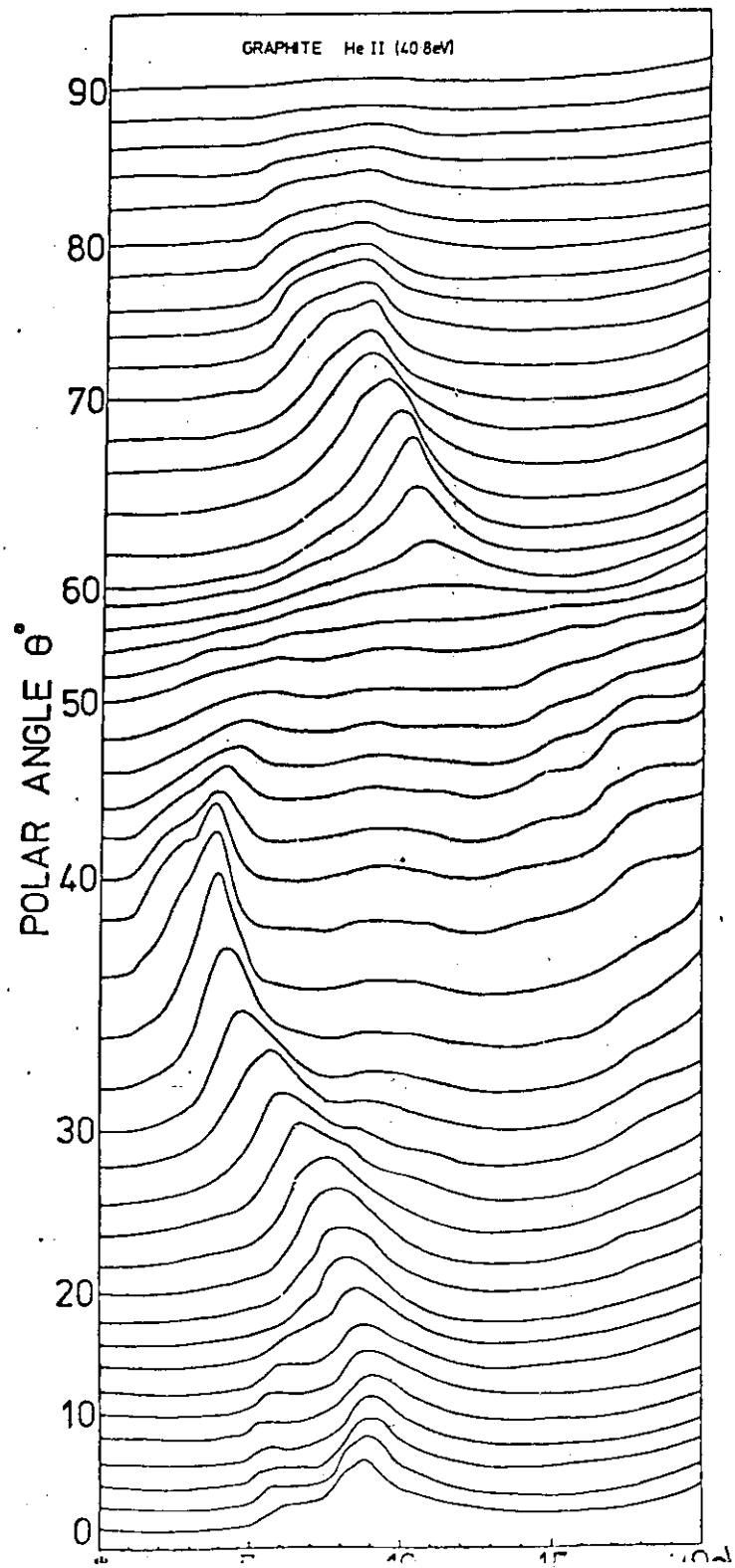

Angular-resolved photoemission (UPS) in graphite.

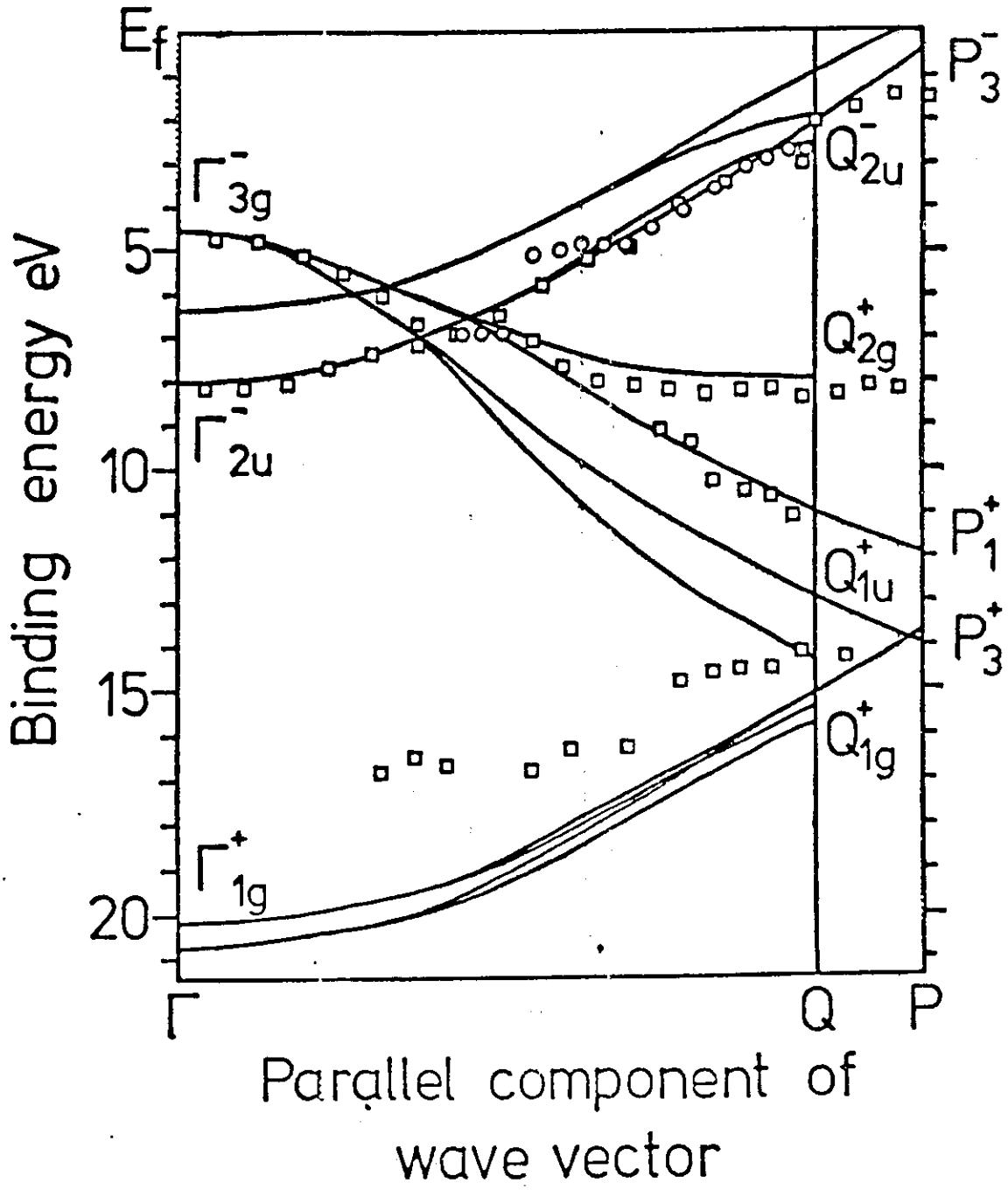

Dispersion of valence bands in graphite: theory (lines), angular-resolved photoemission (squares).

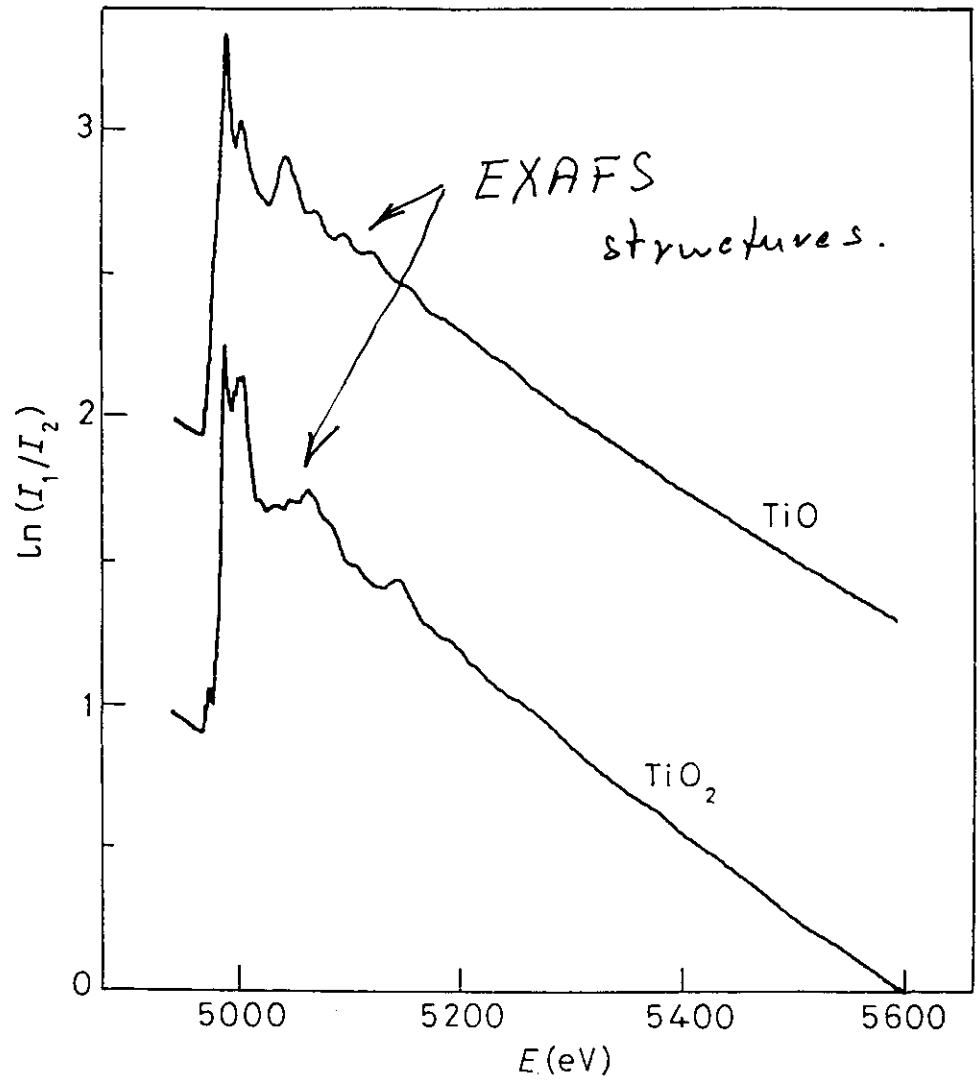

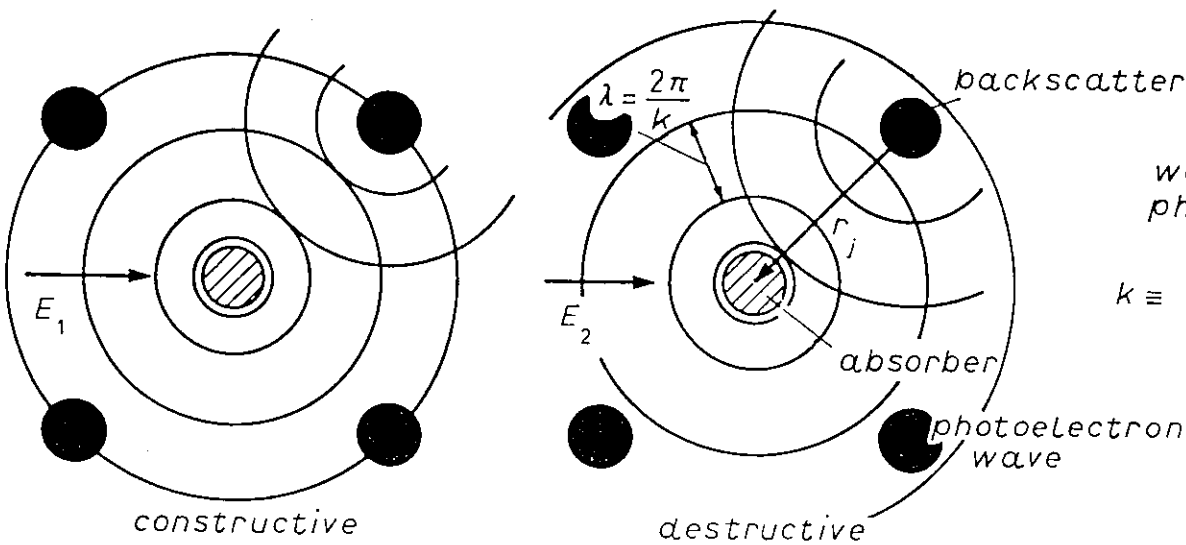

wave vector of photoelectron

$$k \equiv \sqrt{\frac{2m}{\hbar^2}(E - E_0)}$$

Scheme of interference in Extended X-ray Absorption Fine Structure (EXAFS).

EXAFS structure in Ge

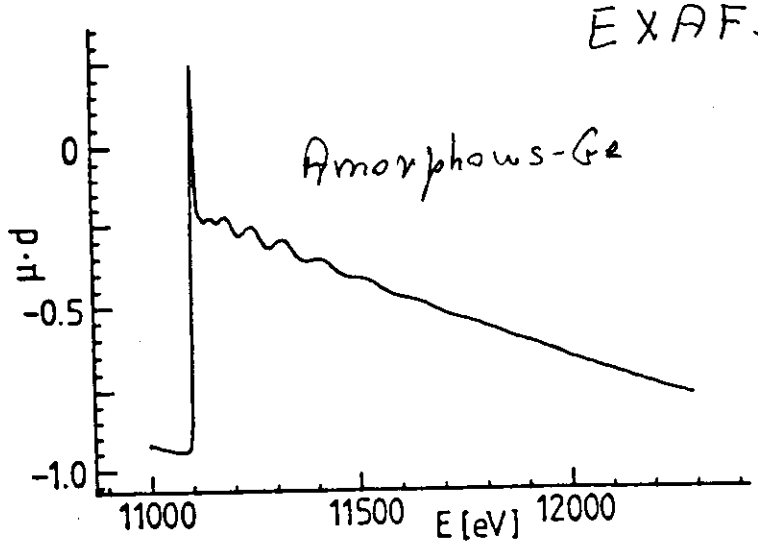

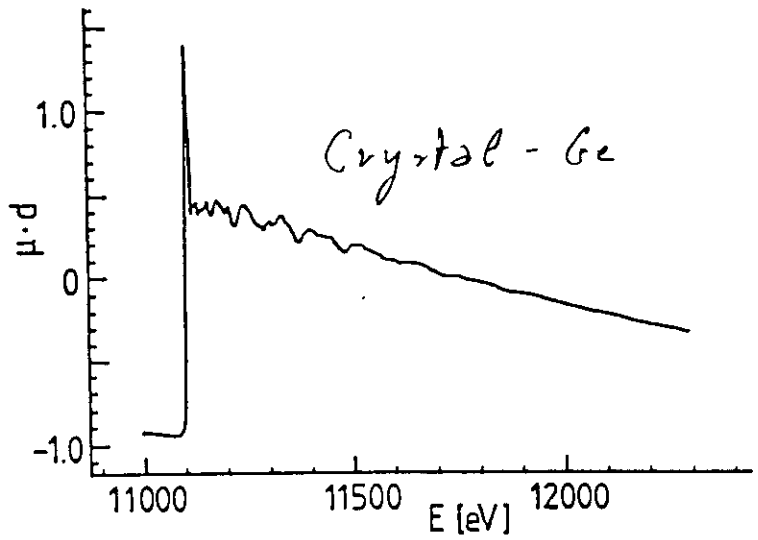

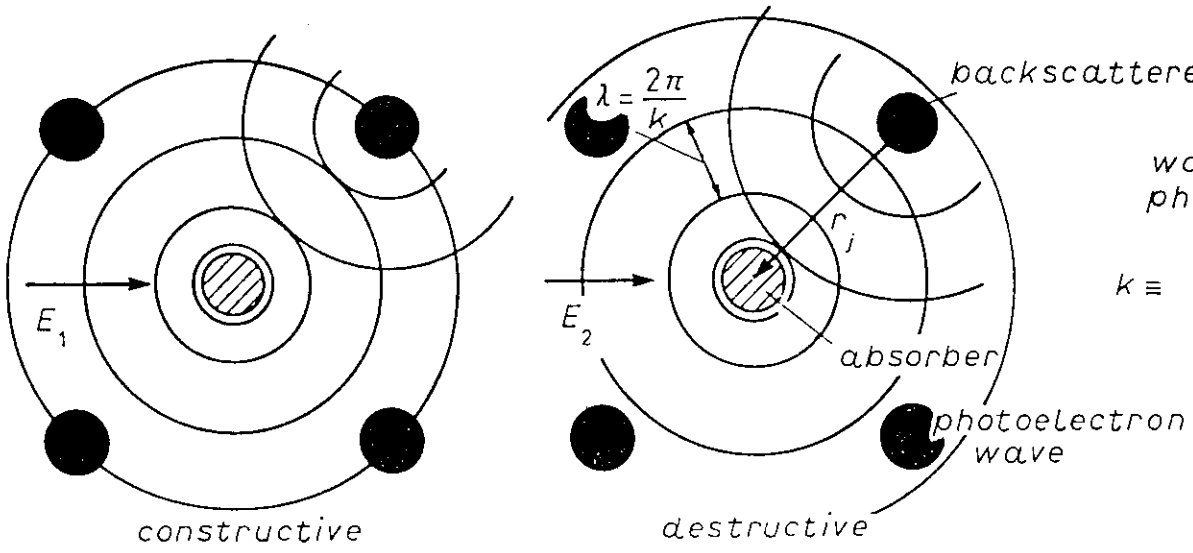

wave vector of photoelectron

$$k \equiv \sqrt{\frac{2m}{\hbar^2}(E - E_0)}$$

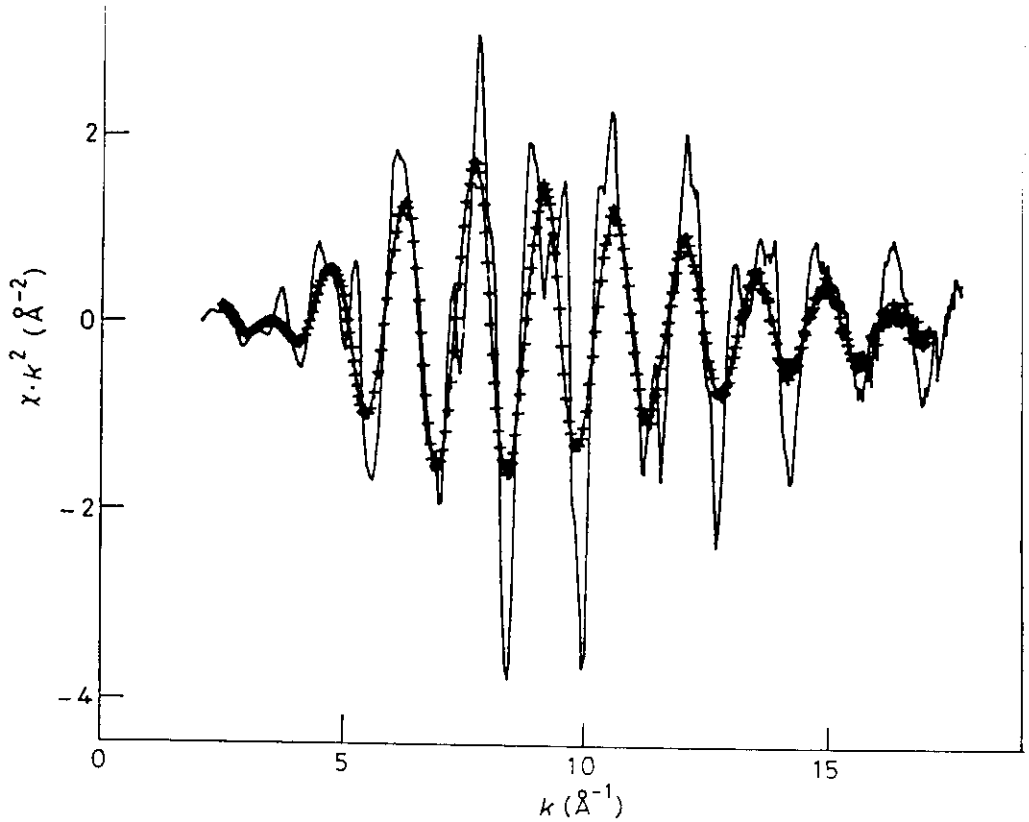

EXAFS $\chi \cdot k^2$ of a-Ge (−+−+−) and c-Ge (——) measured at 77 K

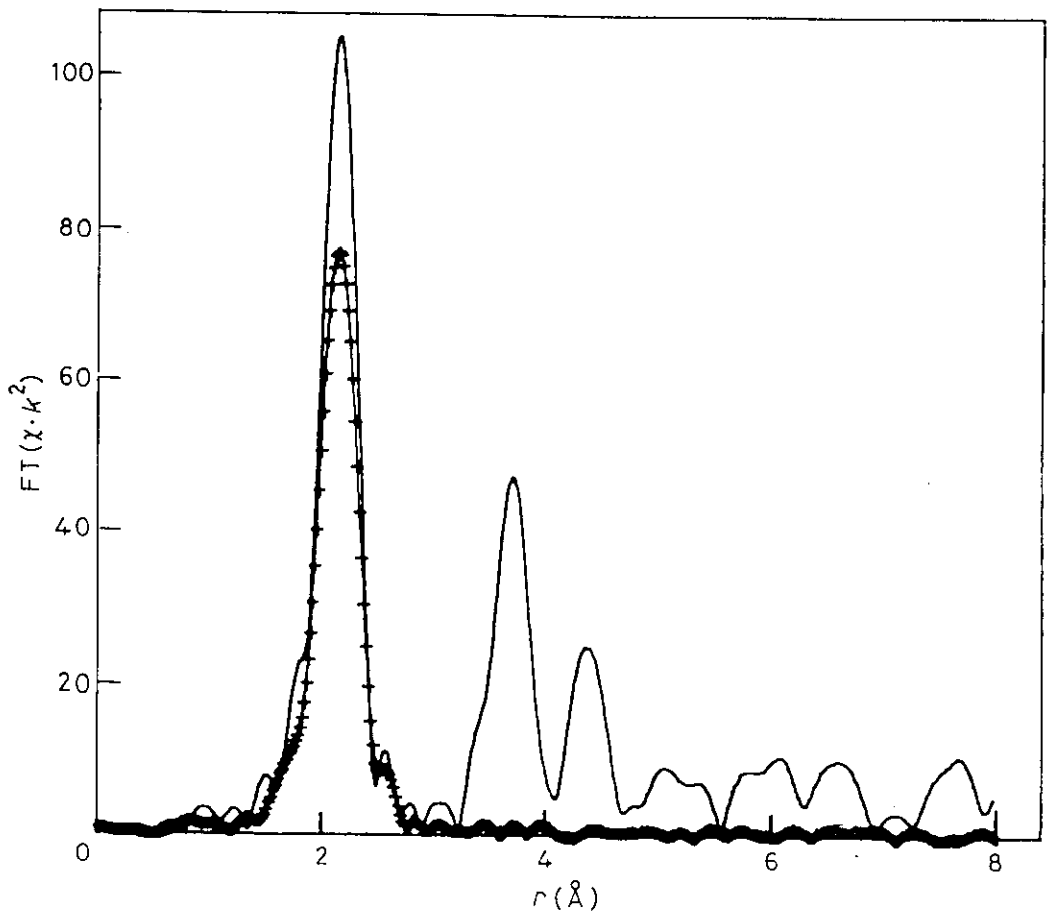

Fourier transforms of the EXAFS of a-Ge (−+−+−) and c-Ge (——)

Data show the radial distribution of neighbours of absorbing atom.

$x = 0.75$ $Ga\,In_3\,As_4$

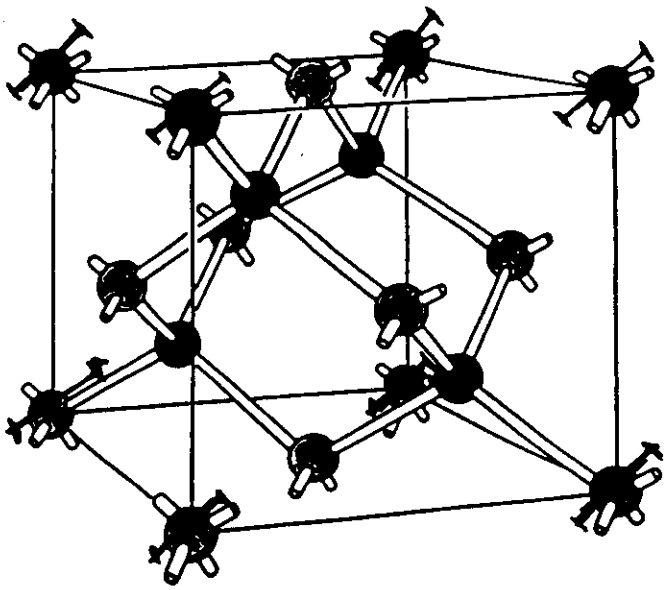

$x = 0.50$

$Ga\,In\,As_2$

$(GaAs)_1(InAs)_1$

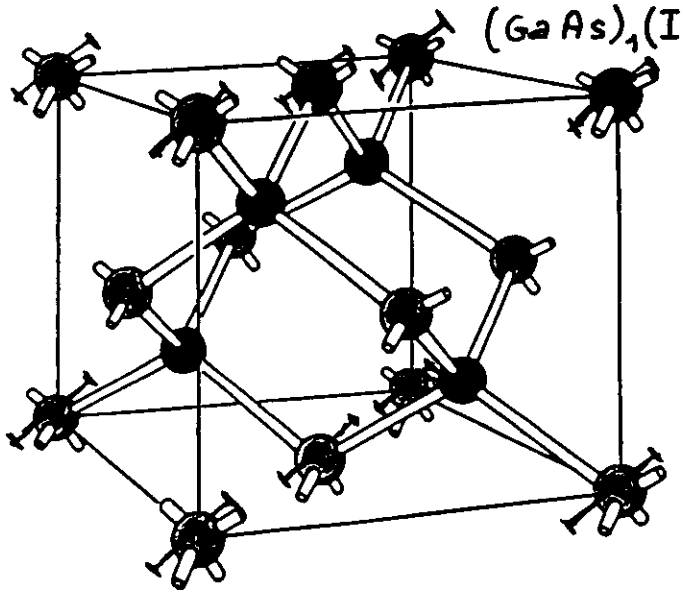

Ga

As

In

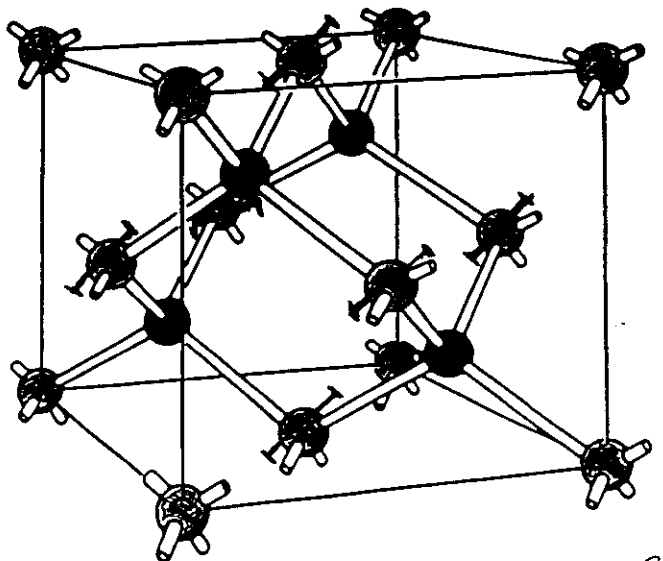

$x = 0.25$

$Ga_3\,In\,As_4$

Atomic distribution in $Ga_{1-x}\,In_x\,As$ alloys for three different compositions.

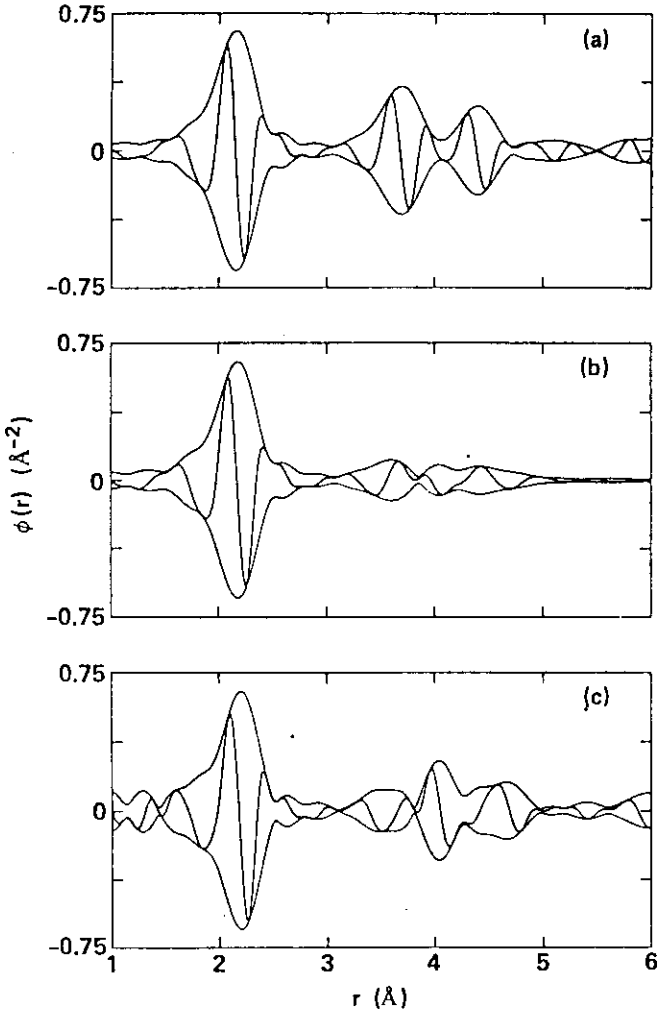

Ga K-edge EXAFS in real space transformed using a window of $k = 3.56$—15.65 Å^{-1} broadened by a Gaussian of width 0.7 Å^{-1} for (a) pure GaAs, (b) $Ga_{0.5}In_{0.5}As$, and (c) $Ga_{0.1}In_{0.9}As$. Note the similarity of the first-neighbor As peak position, width, and amplitude (i.e., similar r, σ, and N). The second-neighbor peaks, on the other hand, are quite different.

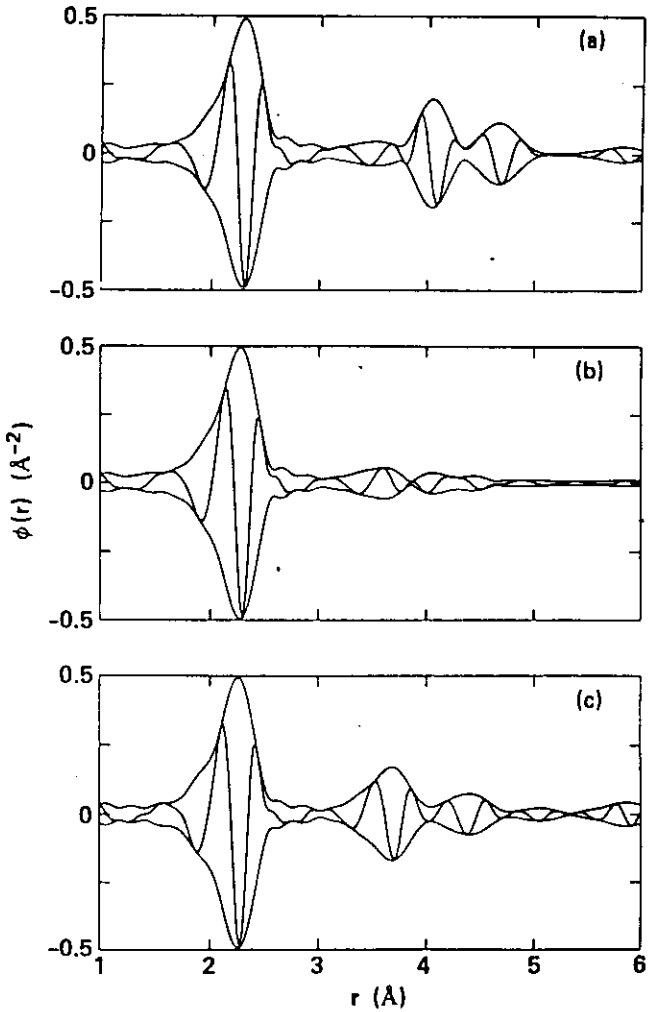

In K-edge EXAFS in real space transformed using a window of $k = 3.96$—18 Å^{-1} broadened by a Gaussian of width 0.7 Å^{-1} for (a) pure InAs, (b) $In_{0.5}Ga_{0.5}As$, and (c) $In_{0.1}Ga_{0.9}As$, all at 77 K. Note the similarity of the first-neighbor As peak position, width, and amplitude (i.e., similar r, σ, and N). The second-neighbor peaks, on the other hand, are quite different.

J. C. Mikkelsen and J. B. Boyce, Phys. Rev. 28, 7130 (1983)

47

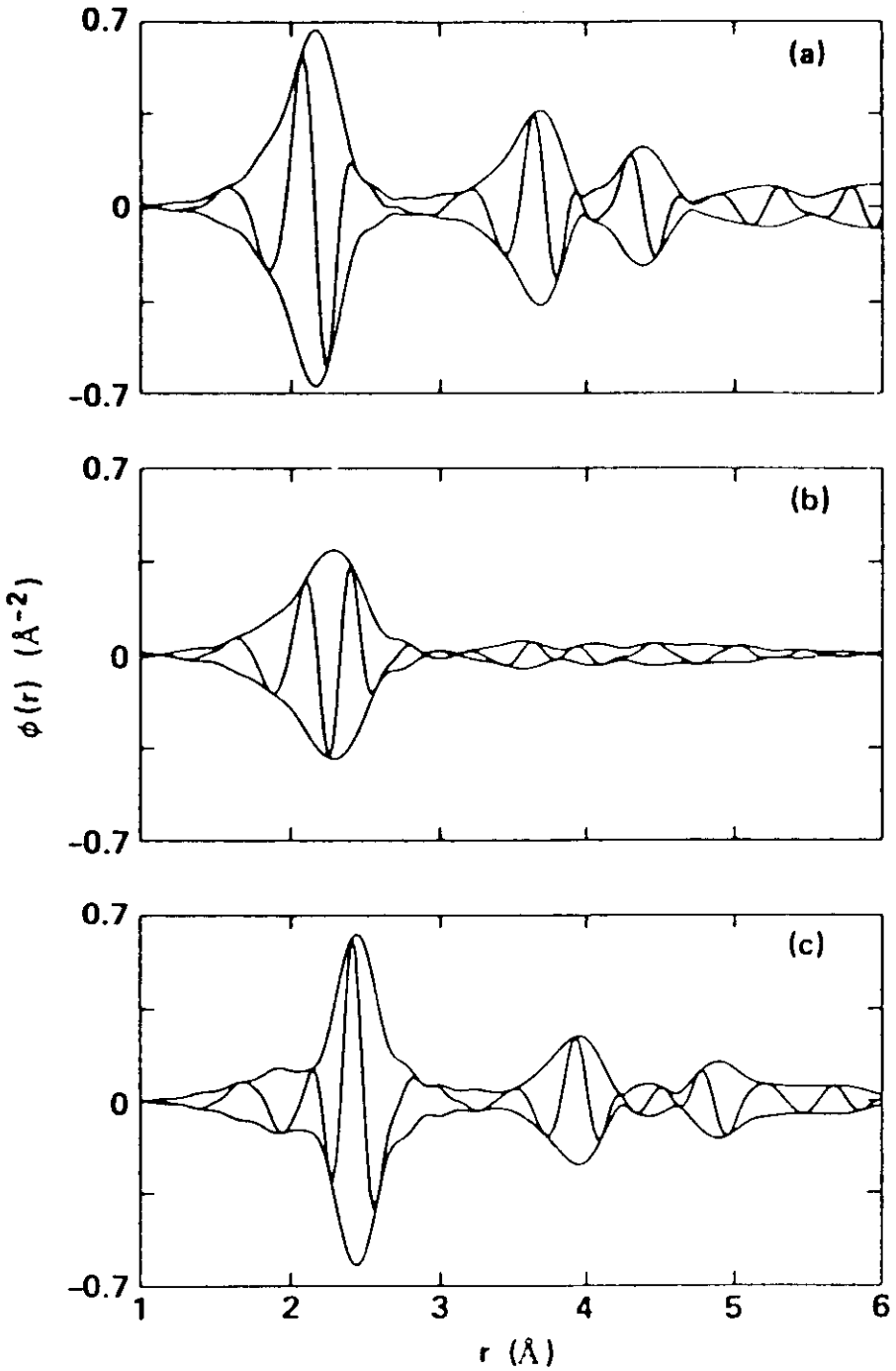

x = 0

x = 0.5

x = 1

FIG. 7. As K-edge EXAFS in real space transformed using a window of 4.16—17.85 Å^{-1} broadened by a Gaussian of width 0.7 Å^{-1} for (a) pure GaAs, (b) $Ga_{0.5}In_{0.5}As$, and (c) pure InAs, all at 77 K. Note that, unlike the cation first-neighbor peaks of Figs. 3 and 4, the first-neighbor peaks here do differ.

$Ga_{1-x}\ In_x\ As$

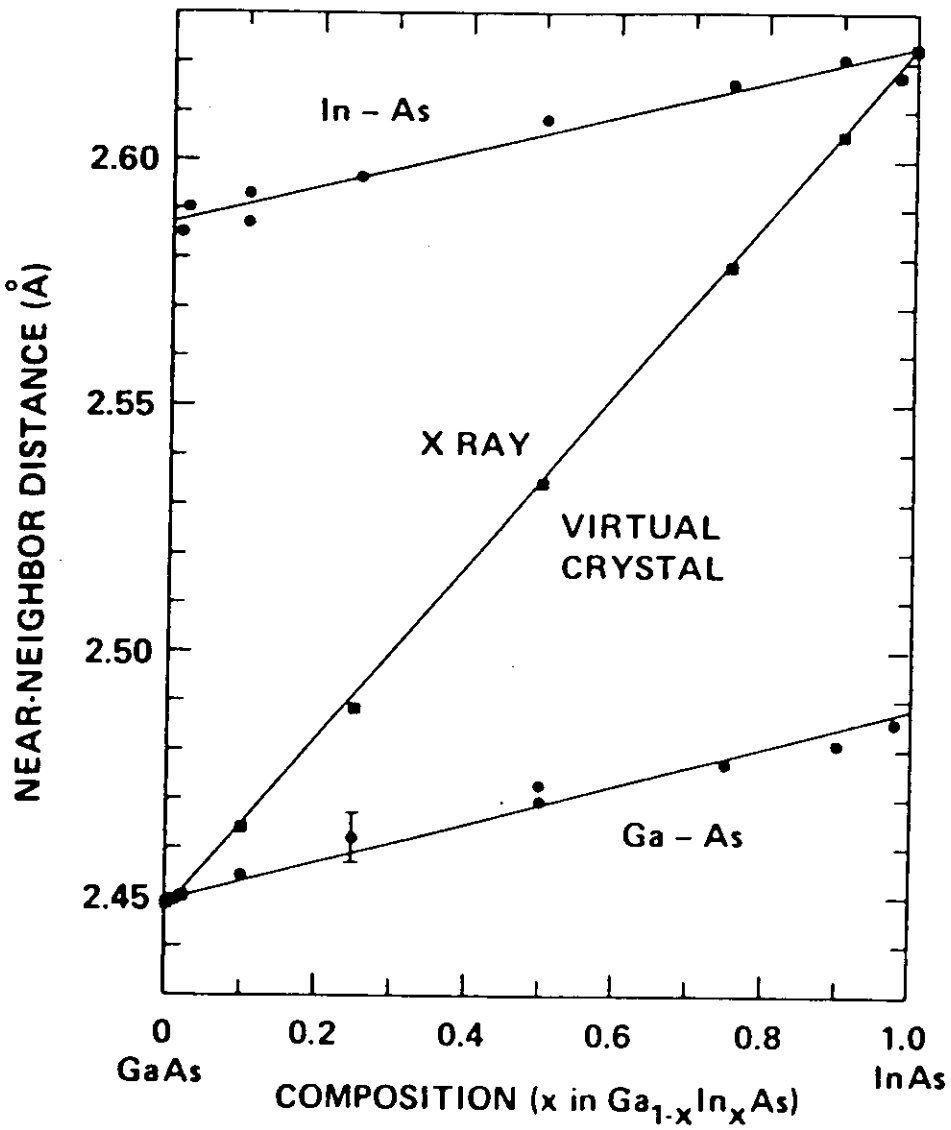

FIG. 6. Ga-As and In-As near-neighbor distances as a function of alloy composition. Middle curve is the VCA cation-anion bond length calculated from the measured x-ray lattice constant. The weighted average of the two NN distances agrees with the VCA (lattice constant) average.

X-ray diffraction ⇒ average distances

EXAFS ⇒ atomic-scale investigation of interatomic distances

J. B. Boyce and J. C. Mikkelsen, Phys. Rev. B31, 6903 (1985)

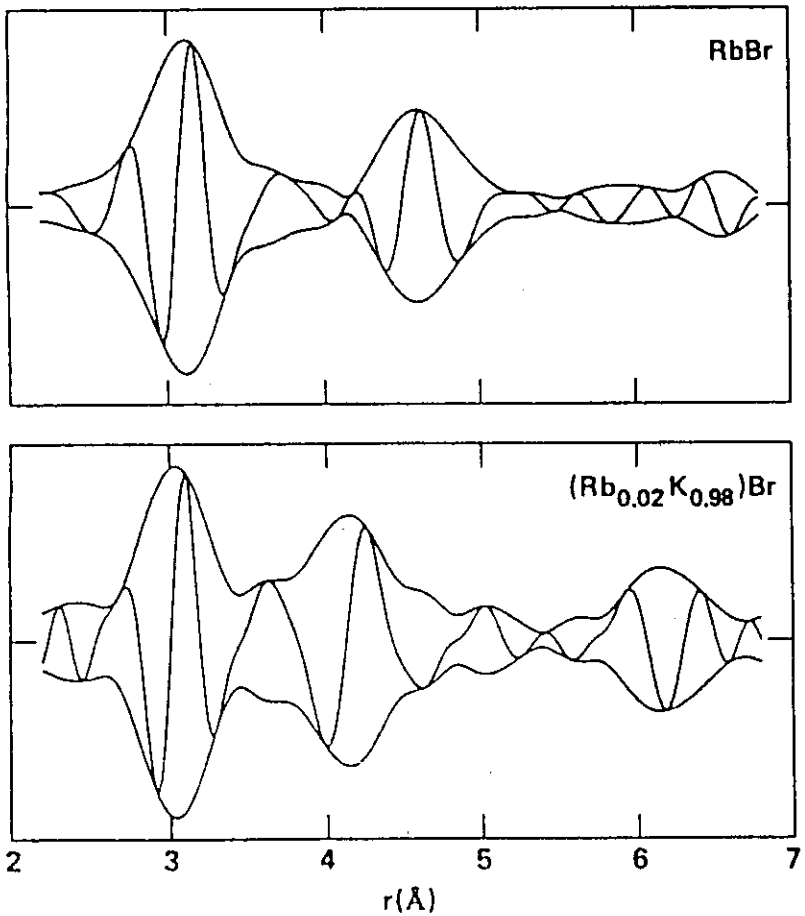

Real part and the magnitude (envelope curve) of the Fourier transform of k times the EXAFS, $\chi(k)$, on the Rb K edge of pure RbBr (upper drawing) and the alloy $(Rb_{0.02}K_{0.98})Br$ (lower drawing), both at 77 K. The data were transformed using a square window form $k = 2$ to 16 $Å^{-1}$, broadened by a Gaussian of half-width 0.7 $Å^{-1}$.

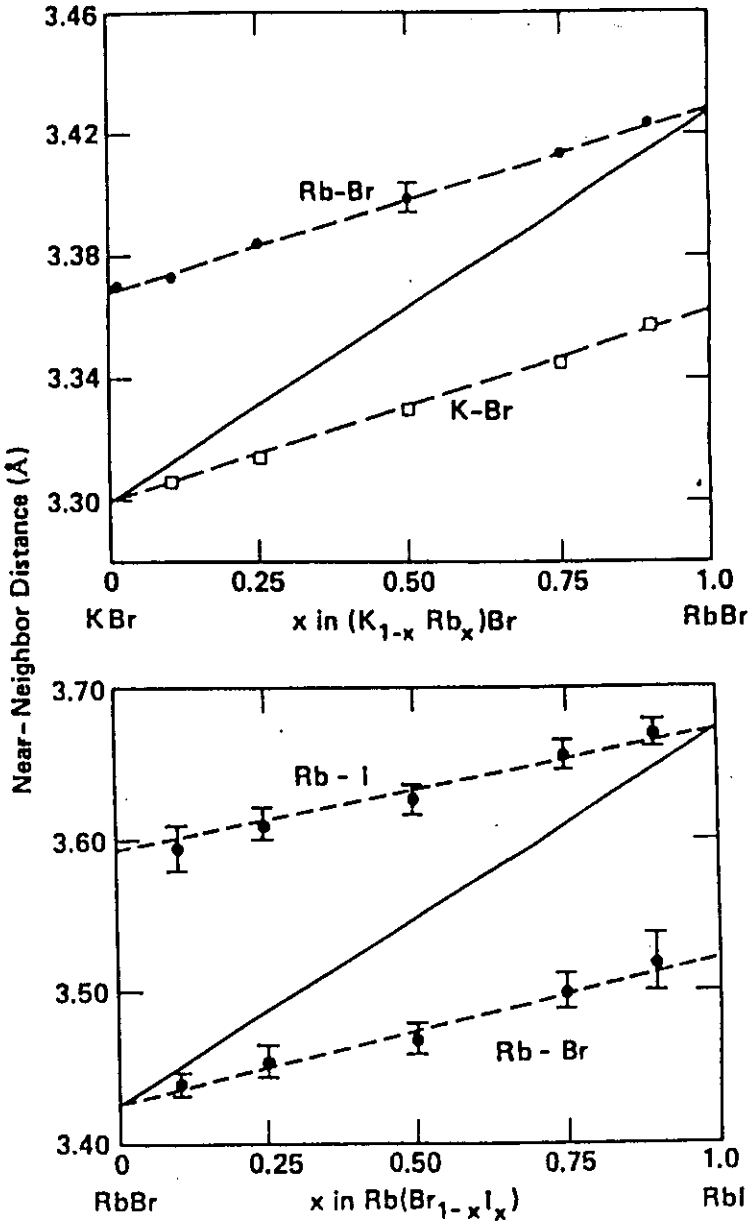

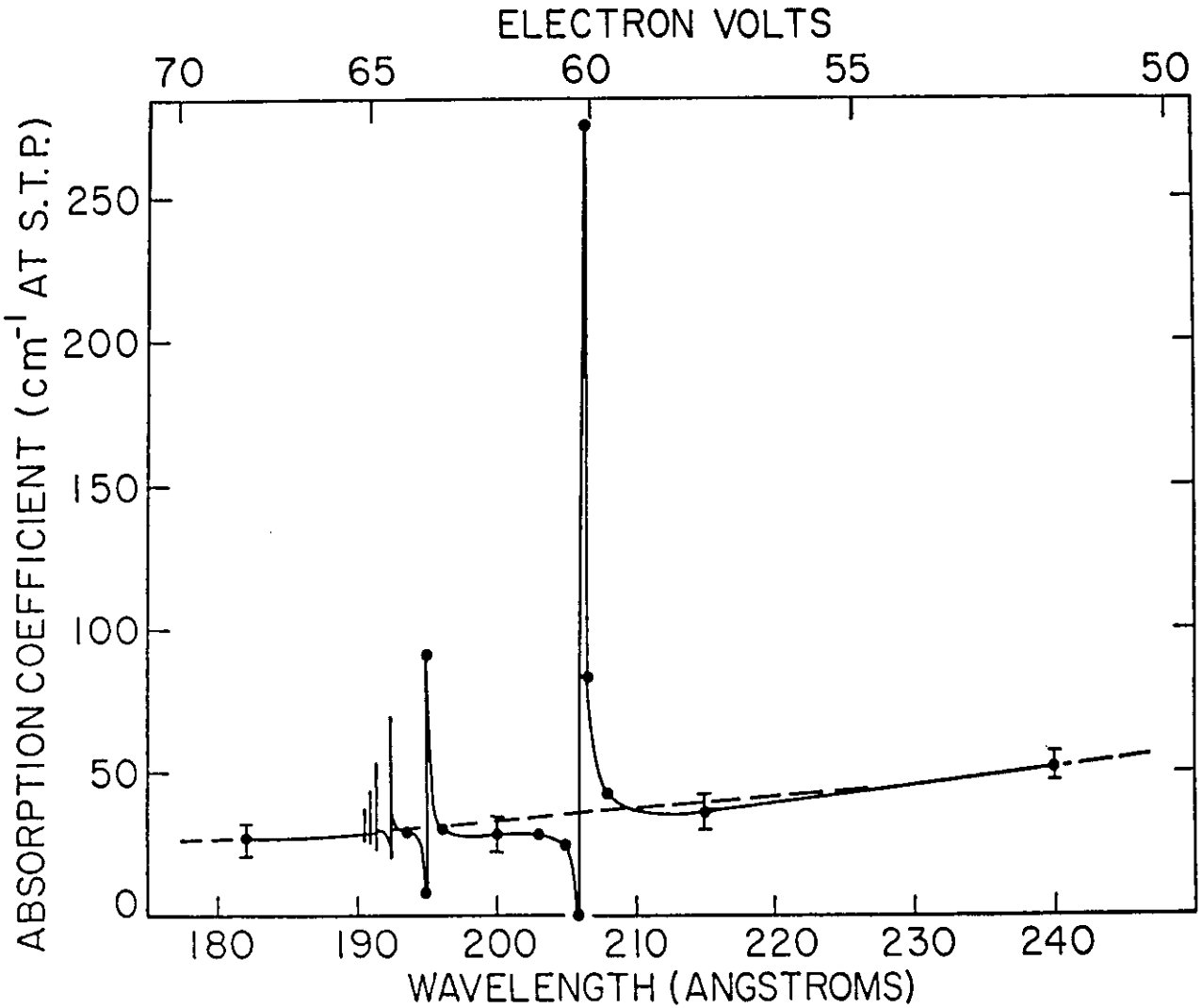

The absorption coefficient of helium in the 175–245-Å region. The solid curve connects the points at which the data were reduced in the present experiment. The dashed curve indicates the result of Lowry *et al.* (1965).

50

Many-electron effects in He: the $2s^1 np^1$ series.

Two-electron absorption.

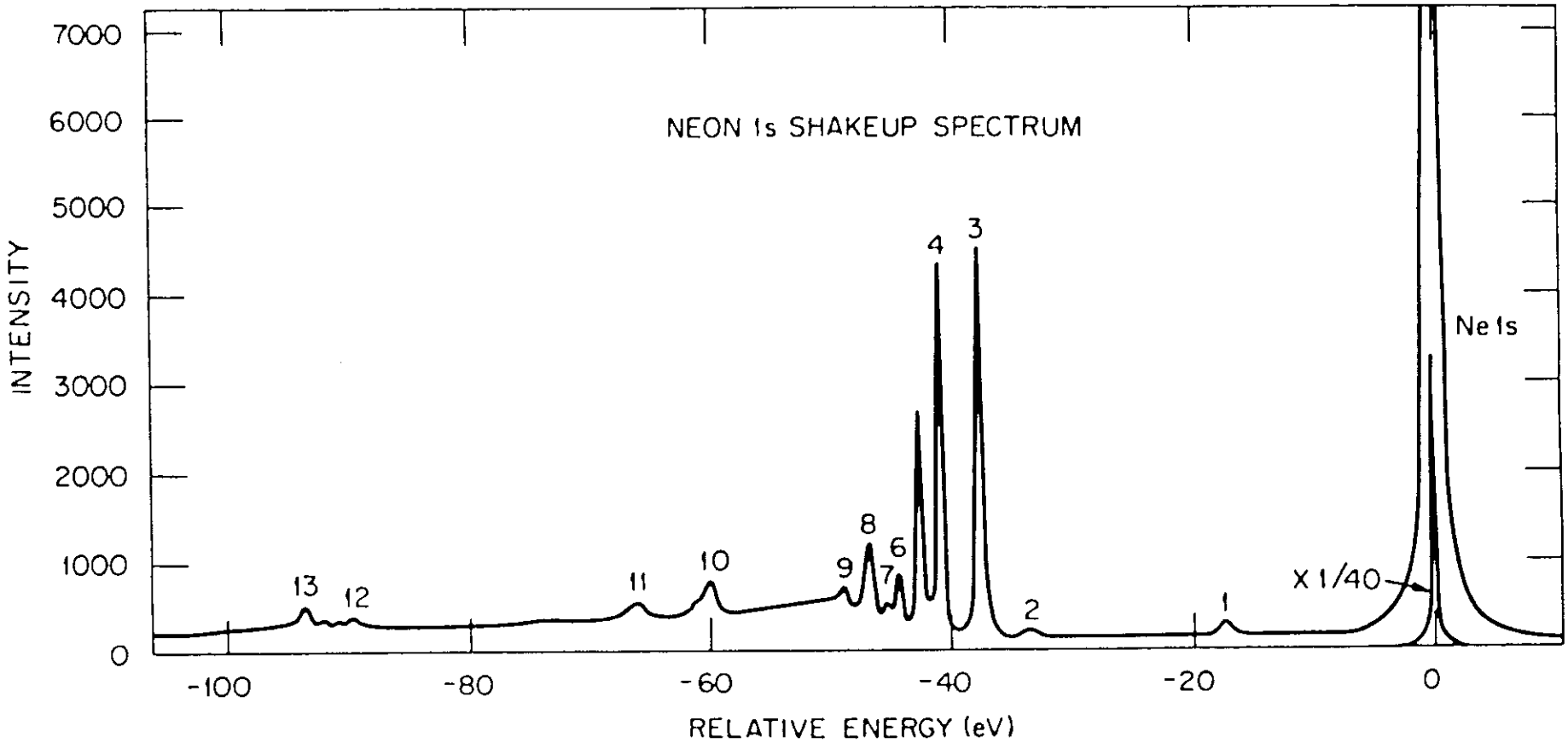

The Ne 1s photoelectron spectrum, showing the single-electron emission photopeak, the shakeup peaks involving (a) a 1s, 2p electron pair (lines 2-9), (b) a 1s, 2s pair (10, 11), and (c) the 1s, $2p^2$ electrons (12, 13), and the KL double-electron ionization continuum (below ΔE=-47eV). Excitation by monochromatized AlKα x rays with a bandwidth of 0.2eV (U. Gelius).

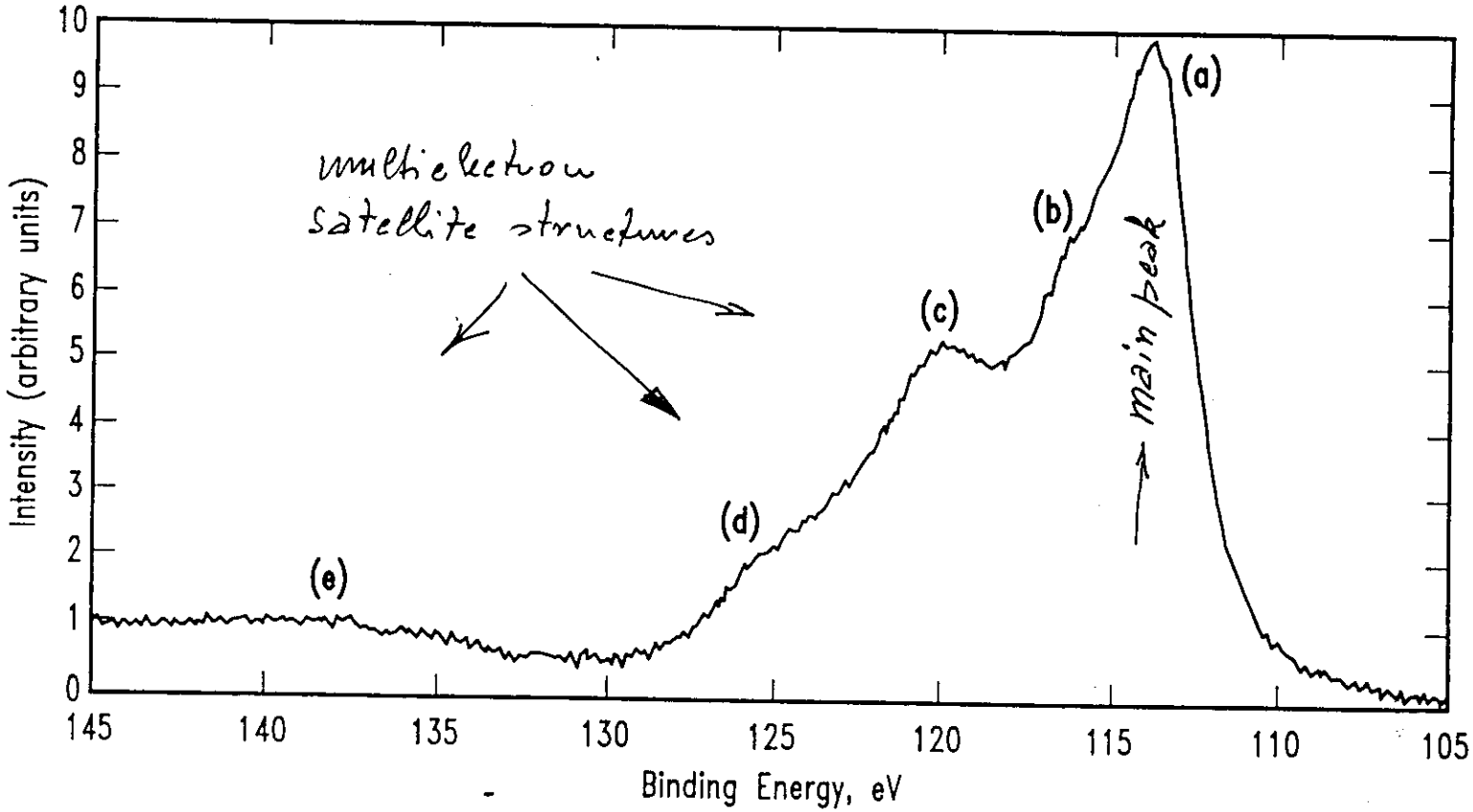

Ni 3s XPS spectrum measured at 80^0 take-off angle on the NiO(100) surface.